

Reproduced with permission of Carol Fulwyler

ELECTRONIC VOLUME ANALYSIS AND VOLUME FRACTIONATION
APPLIED TO MAMMALIAN CELLS

by

Mack Jett Fulwyler

B.S., Idaho State College, 1960

A thesis submitted to the Faculty of the Graduate
School of the University of Colorado in partial
fulfillment of the requirements for the degree of

Doctor of Philosophy

Department of Biophysics

1969

This dissertation has been
microfilmed exactly as received

69-19,535

FULWYLER, Mack Jett, 1936-
ELECTRONIC VOLUME ANALYSIS AND
VOLUME FRACTIONATION APPLIED TO
MAMMALIAN CELLS.

University of Colorado, Ph.D., 1969
Biophysics, general

University Microfilms, Inc., Ann Arbor, Michigan

This Thesis for the Doctor of Philosophy Degree by

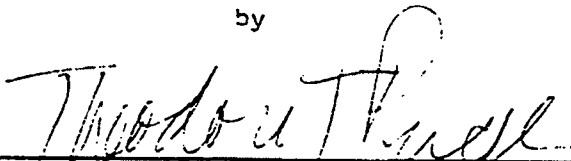
Mack Jett Fulwyler

has been approved for the

Department of

Biophysics

by



Theodore T. Puck



David E. Pettijohn

Date 5-13-69

Fulwyler, Mack Jett (Ph.D., Biophysics)

Electronic Volume Analysis and Volume Fractionation Applied to Mammalian Cells

Thesis directed by Professor Theodore T. Puck

The principle and apparatus of electronic cell volume analysis and of a newly developed electronic cell separator capable of fractionating cells according to differences in volume are described. The apparatus have been applied to the study of normal and abnormal human leucocytes, and a correspondence between cell volume and cell type has been obtained. Abnormal volume distributions of infectious mononucleosis, acute lymphoblastic leukemia, and chronic lymphocytic leukemia are presented and compared with normal.

An analysis of mouse bone marrow is described which leads to a correlation of cell volume with cell type. The effect of X irradiation on the volume distributions of bone marrow and spleen is shown, and the rate of cell loss for several volume ranges is given.

Colony-forming units (CFU) found in mouse bone marrow and spleen have been studied, and a volume distribution of these stem cells in bone marrow is given. CFU's were found to be most abundant in the volume range occupied by granulocytes and not in the volume range wherein most lymphocytes are found, thus arguing against the idea that CFU are small lymphocytes as some workers have suggested.

The effect of development of early AKR leukemia on the volume distribution of mouse spleen cells is shown. Further, it is shown that the enlarged, transformed cells found in the spleen are able to initiate leukemia in a recipient mouse whereas the smaller, normal cells of the same spleen are not.

This abstract is approved as to form and content. I recommend its publication.

Signed Theodore P. Kutz

Faculty member in charge of dissertation

ACKNOWLEDGEMENTS

The biological research reported here was performed under the supervision of Professor Theodore T. Puck. Development of instrumentation was supervised and supported by Dr. Wright H. Langham of the Los Alamos Scientific Laboratory. Encouragement by these two individuals has been primarily responsible for my graduate education.

Credit must be given to Mr. T. Carroll and Mr. J. Coulter for aid in mechanical design and construction. The majority of the electronics were designed by Dr. R. D. Hiebert and Mr. R. B. Glascock of the Los Alamos Scientific Laboratory. The pulse control and delay logic system was the product of a joint effort by myself, R. B. Glascock and by Mr. N. Johnson of the Biophysics Department, University of Colorado.

Special thanks must be given to Mr. Paul Wuthier for his efforts to elevate my understanding of mammalian cell biology. Essentially all of the experimental work with mouse cells was carried out under his immediate supervision. Development of a volume-stabilizing medium for use with mouse cells is his work, as is the technique to obtain photomicrographs of separated cells.

In spite of the heavy cost to her, my wife has been steady in her support and encouragement. Whatever success I may achieve is equally her success.

TABLE OF CONTENTS

Chapter	Page
I. INTRODUCTION.....	1
II. APPARATUS, METHODS, AND MATERIALS.....	5
A. Physical Apparatus and Methods.....	5
1. Electronic Volume Sensing.....	5
a. Principle.....	5
b. Apparatus.....	7
2. Electronic Sorting of Cells According to Difference in Volume.....	10
a. Operation and Construction.....	10
<u>1.</u> Volume Sensor and Droplet Generator...	12
<u>2.</u> Droplet Formation and Charging.....	14
<u>3.</u> Separation and Timing Considerations..	17
b. Electronics.....	19
<u>1.</u> Droplet Production.....	19
<u>2.</u> Droplet Deflection.....	21
<u>3.</u> Volume Sensing.....	21
<u>4.</u> Particle Detection and Selection.....	21
<u>5.</u> Pulse Control and Delay.....	22
<u>6.</u> Droplet Charging.....	25
B. Biological Methods and Materials.....	26
1. Volume Analysis of Human Leucocytes in Peripheral Blood.....	26
a. Concentration of Leucocytes.....	26
b. Microscopic Examination of Separated Cells.....	26
2. Cell Volume in Mouse Hemopoiesis.....	27
a. Preparation of Cell Suspensions.....	27
b. Titration of CFU.....	28
c. Microscopic Examination of Separated Cells.....	29
d. Differential Counting of Cell Types.....	29

III. RESULTS.....	30
A. Volume Analysis and Particle Separation.....	30
1. Polystyrene Spheres.....	30
2. Mixture of Human and Chicken Erythrocytes.....	30
B. Application to Biological Problems.....	33
1. Development of a Volume-Stabilizing Medium....	33
2. Viability of Separated Cells.....	36
3. Volume Analysis of Human Leucocytes in Peripheral Blood.....	37
a. Normal Human Leucocytes.....	38
b. Abnormal Human Leucocytes.....	41
4. Cell Volume in Mouse Hemopoiesis.....	45
a. Volume Analysis of Normal Mouse Bone Marrow and Spleen.....	45
b. Effect of X Irradiation on Volume Distri- bution of Bone Marrow and Spleen.....	52
c. Colony-Forming Units in Bone Marrow and Spleen.....	55
d. Spleen Cell Volume in AKR Mouse Leukemia..	61
IV. DISCUSSION.....	66
A. Volume Analysis and Cell Separation.....	66
1. Minimum Sensible Volume.....	66
2. Resolution of Separation.....	66
3. Limitation on Rate of Analysis.....	66
4. Extension to Other Sensors.....	67
B. Biological Applications.....	69
1. Human Leucocytes.....	69
2. Cell Volume in Mouse Hemopoiesis.....	70
a. Normal Mouse Bone Marrow.....	70
b. Effect of X Irradiation on Bone Marrow and Spleen.....	70
c. Colony-Forming Units in Bone Marrow and Spleen.....	71
d. Spleen Cell Volume in AKR Mouse Leukemia..	76

V. CONCLUSION.....	77
VI. FOOTNOTES AND BIBLIOGRAPHY.....	78

LIST OF TABLES

	Page
Table I Human Leucocyte Separation: Cell Types Present in Three Areas of the Volume Distribution.....	41
Table II Differential Count, CFU Titer, and Percent of Total CFU of Gross Suspension and of Fractions 1L, 1R, 2L, and 2R.....	60
Table III Cell Volume and Induction of Leukemia in AKR Mice.....	65

LIST OF FIGURES

		Page
Figure 1	Volume distribution of mouse bone marrow cells (689704).....	9
Figure 2	The electronic cell separator (685151).....	11
Figure 3	Simplified cross-sectional illustration of the volume sensor and droplet generator (684277).....	13
Figure 4	Droplet formation and deflection (680507).....	15
Figure 5	Block diagram of the electronics system (680690)..	20
Figure 6	Pulse control and delay logics (680689).....	23
Figure 7	Fractionation of polystyrene spheres of 6-14 μ diameter (681239).....	31
Figure 8	Volume distribution of a mixture of human and chicken erythrocytes (659467).....	32
Figure 9	Photomicrographs of a mixture of human and chicken erythrocytes and of 2 separated fractions (6801072).....	34
Figure 10	Volume distributions of bone marrow cells at various times after dispersion (689698).....	35
Figure 11	Volume distribution of normal human leucocytes (689705).....	39
Figure 12	Photomicrographs of separated cell fractions compared with the original sample (67837).....	40
Figure 13	Volume distribution of leucocytes from a patient having infectious mononucleosis (689695).....	42
Figure 14	Cells isolated from peripheral leucocytes of a patient having infectious mononucleosis (6810642).....	43
Figure 15	Volume distribution of leucocytes in infectious mononucleosis compared with normal leucocytes (659628).....	44
Figure 16	Volume distributions of leucocytes from peripheral blood of a normal person and a person having acute lymphoblastic leukemia (659625).....	46

Figure 17	Volume distributions of leucocytes from peripheral blood of a normal person and a person having chronic lymphocytic leukemia (659624).....	47
Figure 18	A typical volume distribution of mouse bone marrow cells (689701).....	48
Figure 19	Frequency distribution of cell types in bone marrow volume distribution (689702).....	50
Figure 20	Volume distribution of normal mouse spleen and marrow cells (689700).....	51
Figure 21	Effect of X irradiation on volume distribution of spleen cells (689699).....	53
Figure 22	Effect of X irradiation on volume distribution of bone marrow cells (689703).....	54
Figure 23	Bone marrow cell loss following X irradiation (689706).....	56
Figure 24	Volume distributions of the gross marrow cell suspension and the 2 isolated fractions 1L and 1R (689696).....	57
Figure 25	Volume distributions of the gross bone marrow suspension and the 2 isolated fractions 2R and 2L (689697).....	59
Figure 26	Volume distributions of spleen cells from normal and leukemic AKR mice (6810520).....	62
Figure 27	Volume distributions of separated fractions and the gross spleen cell suspension from a leukemic AKR mouse (6810521).....	63
Figure 28	CFU abundance within the volume distribution of mouse bone marrow (689707).....	74

I. INTRODUCTION

Much of the complexity of research in cell biology is a result of the heterogeneity of cell populations. The ability to isolate a reasonable number of cells, homogeneous in some property, would certainly be of value.

In the past many methods of cell separation have been tried including those based on the following techniques: absorption (1), flotation (2), agglutination and sedimentation (3), magnetic susceptibility (4), electrophoretic mobility (5), electromagnetic interaction (6), and recently counter-current distribution (7). Centrifugation techniques have been developed to the point where a partial separation of the different human white blood cell types can be obtained (8). Goodman has described her method of separation of mouse bone-marrow cells using density gradient centrifugation (9). More recently a paper has appeared describing separation of Guinea-pig bone marrow cells using a 1-g sedimentation system (10). This latter technique appears to offer a promising method of cell separation which is jointly dependent on cell volume and density, although primarily on the former; however, from the data presented it is not yet possible to evaluate the resolution limits of this technique.

All of these techniques are unsatisfactory in one or more of the following ways: a) The cell property upon which they operate is often ambiguous or of questionable biological significance. b) Cell viability is often adversely affected by technical requirements of the process. c) The degree of homogeneity obtained within an isolated fraction is unsatisfactory.

Electronic separation of biological cells was first announced by this author in 1965 (11). Somewhat later (1967) a similar technique involving electronic cell sensing was announced by Kamentsky, et al. (12). A brief description of this technique is called for because of its similarity to the system to be described. In the Kamentsky system, cells, in suspension, flow through a small channel which is illuminated with ultraviolet light. Absorption of 2537 Å light by nucleic acids attenuates the transmitted beam. A photomultiplier tube produces an electronic pulse which is a measure of the degree of attenuation. Pulses of a certain amplitude class will activate a motor-driven syringe causing an increment of flowing liquid containing the desired cell to be drawn into a side channel. This system has two primary faults. Although the amount of liquid pulled into the side channel is small (0.03 μ l) it is still likely to contain several cells in addition to the one desired, so that purity is low. Also, because of the inherent inertia of motors or other mechanically activated systems, the separation rate is limited to perhaps 500 operations per second.

The electronic cell separator to be described here, is a new approach to the problem of cell fractionation. A primary advantage of this technique over nonelectronic systems is that, in theory, individual cells can be analyzed and separated on the basis of one or a combination of electronically measureable characteristics. Separation is achieved without mechanical motion and the minimum amount of liquid which can be isolated is one droplet, having a volume of about 10^{-6} ml; consequently, the rate of cell analysis, rather than separation, is the predominant limiting factor.

It is the objective of this thesis to describe the principles and apparatus of electronic cell volume analysis and electronic cell separation and to present the results of application of these techniques to an increasingly complex series of mammalian cell systems. Artificial mixtures of human and chicken erythrocytes are fractionated, illustrating the ability of the instrument to isolate pure fractions of biological cells of differing volume. The volume distribution of normal human leucocytes is obtained, and the structure within the distribution is identified with specific cell types. Volume distributions of abnormal leucocytes, obtained from persons having infectious mononucleosis, acute lymphoblastic leukemia, or chronic lymphocytic leukemia, are given illustrating the changes in leucocyte volume which accompany these diseases. The apparatus is also applied to the study of hemopoiesis in the mouse, establishing the relationship between cell volume and cell type within normal mouse bone marrow. Volume analysis is applied to mouse spleen, illustrating the differences in lymphocyte volume between this tissue and bone marrow. Cell loss from mouse bone marrow and spleen following X irradiation is studied, showing that lymphocytes are the first cells to be lost. The volume distribution of colony-forming units (CFU) in mouse bone marrow and spleen is obtained, indicating that the majority of these stem cells are found in the volume range of granulocytes and that few are associated with small lymphocytes as had previously been thought. Development of early leukemia in AKR mice is correlated with alterations in spleen cell volume, and it is shown that the enlarged, transformed cells are capable of inducing leukemia in host mice whereas the cells with normal volumes are not. Exten-

sion of electronic cell analysis and separation to other sensors is discussed along with the limitations of the system as it now exists.

II. APPARATUS, METHODS, AND MATERIALS

A. Physical Apparatus and Methods

1. Electronic Volume Sensing

a. Principle

With the development of the Coulter Counter (13), it became possible to measure the concentration of microscopic particles in liquid suspension. This device operates by isolating, with a dielectric material, two volumes of electrically conducting liquid. Contained in this dielectric wall is an orifice connecting the two liquid reservoirs and through which the cell suspension is caused to flow by imposing a negative pressure (vacuum) on one side. By proper adjustment of concentration, particles pass through the aperture one at a time. An electric potential, impressed across platinum electrodes immersed in each reservoir, causes current to flow through the orifice. Entry of a particle having conductivity different than that of the suspending liquid produces a disturbance in the flow of electric current. By counting the number of disturbances (electric pulses) corresponding to passage of a known volume of suspension, particle concentration is obtained. The usefulness of the device is greatly increased because the change in current is related to the volume and shape of the particle. The dependence of current change on these properties has been studied in considerable detail by others (14,15). For spherical particles the change in electrical resistance of the aperture contents, corresponding to the presence of a nonconducting particle, is:

$$R = y(3/2)v/A^2,$$

where v = particle volume, A = cross-sectional area of the orifice, and y = solution conductivity. This equation was experimentally determined using a scaled-up model of the Coulter aperture and is based on the assumption that the resistance-capacitance time constant of the cell is much less than the rise time of the associated electronics (14). The time constants for most cells are on the order of $1 \mu\text{sec}$, compared to an amplifier integrating time of approximately $5 \mu\text{sec}$. An additional assumption is that the radius of the particle is much less than the radius of the aperture. This expression is expected to hold for spheroids but not for short rods or discs. Essentially, the Coulter sensing principle measures the volume of conducting liquid from which the electric current is excluded. This exclusion may be due to physical displacement of conducting liquid by the nonconducting particle or to electric current lines avoiding the conducting liquid contained within an indentation of the particle surface if an alternate path of lower electrical resistance is available. A very thin disc having a diameter four times its thickness and moving through the orifice with its axis parallel to the axis of the aperture will produce a resistance change twice that produced by a sphere of equal volume. This difference is due to an edge effect by which the electric current flow avoids the liquid near the center of each face of the disc. Passing through edge-on, the same disc will produce a resistance change approximately equal that of the equivalent sphere. Fortunately, most mammalian cells, with the exception of erythrocytes, are spheroidal when in free suspension and lend themselves to accurate volume determination by this method. Hydrodynamic shear within the orifice causes erythrocytes to orient

edge-on when entering the aperture and thus gives a resistance change approximately equal that of a sphere of equivalent volume. The rounded edges of the red cell further minimize end effects in the edge-on orientation.

The accuracy of relative volume measurement has been shown to be quite high. Kubitschek (16) determined the relative diameters of 1.3- μ and 1.67- μ polystyrene-latex spheres by optical microscopy and by sedimentation in a sucrose gradient. The particles were then electronically measured using the Coulter principle and gave the expected volume ratio to within 1%. Using a variety of mammalian tissue culture cell lines, Anderson and Petersen (17) have compared modal volume, as determined by optical measurement of cell diameter, with that given by electronic measurement. These populations of cells were randomly growing; their diameters were measured as they normally occur in suspension culture and also after swelling in hypotonic medium. The latter treatment serves to distend the cells into spheres, facilitating accurate measurement of diameter. These studies indicate that the electronically determined modal volumes have an absolute error of less than 10%. In the work presented here, the apparatus were calibrated primarily against 3.04- μ diameter polystyrene-latex spheres (18) and secondarily against human and mouse erythrocytes. Shape effects were assumed to be small and were ignored. Most of these distributions were obtained using a sensing orifice 50 μ in diameter and approximately 225 μ in length.

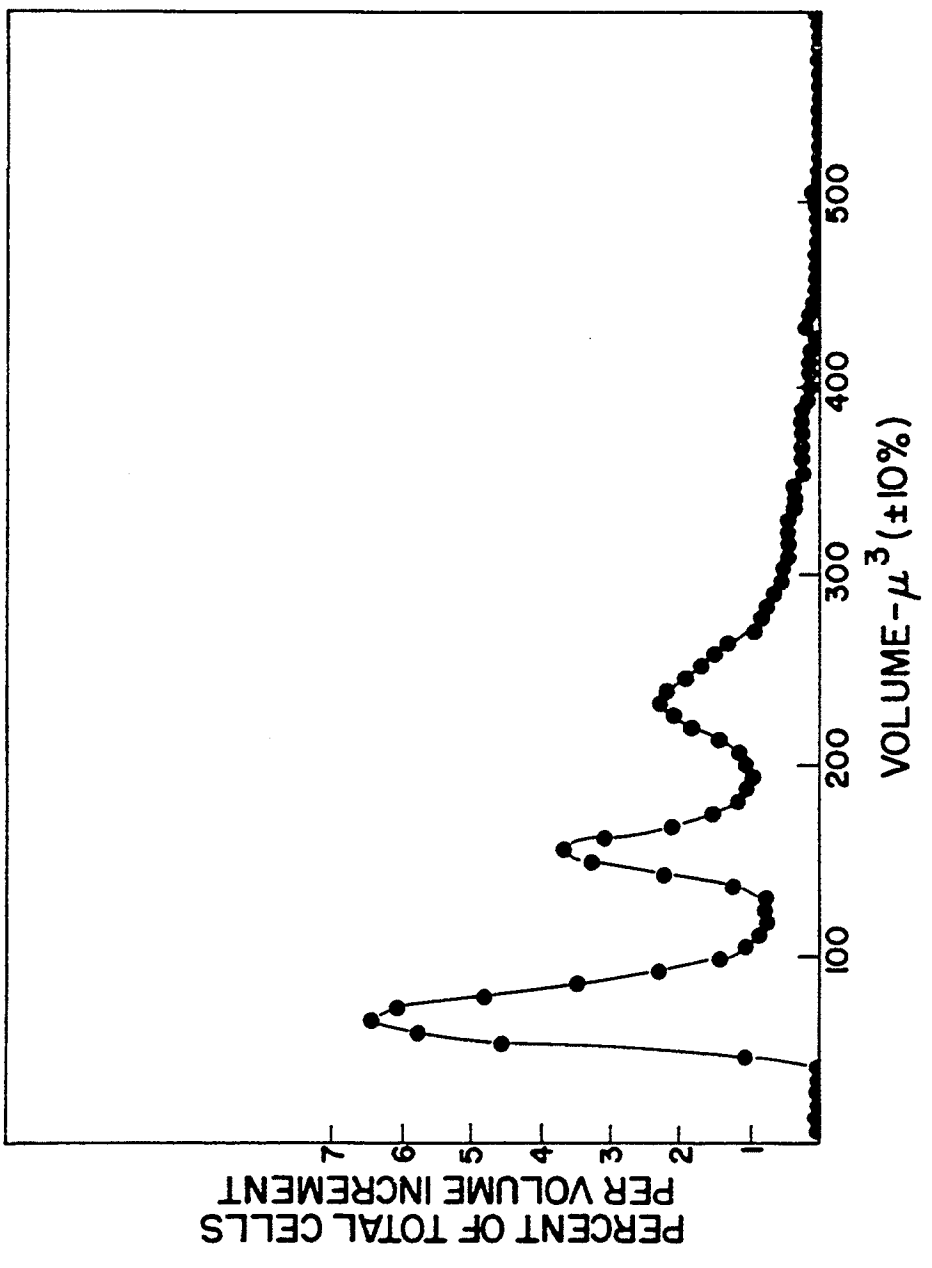
b. Apparatus

The aperture constant-current supply consists of a simple

high-voltage source using large resistors to provide between 10 and 200 μA . Amplification of the particle pulse takes place in three sections. The preamplifier (19) is a low-noise, current sensitive device of less than 1000 Ω input impedance, making the output insensitive to changes in solution conductivity (14). Transimpedance e_o/i_n , a measure of the amplification occurring during conversion of a current pulse (i_n) to a voltage pulse (e_o), is 300 $\text{k}\Omega$. The main pulse-amplifier (19) consists of two feedback amplifier sections operated in series. Each section has a maximum gain of 100 and incorporates integrating and differentiating networks empirically selected to give the best signal-to-noise ratio. For typical pulses having rise times of about 10 μsec and durations greater than 20 μsec , these time constants are 5 and 50 μsec , respectively. The magnitude of these amplified pulses is proportional to the resistance change associated with a particle in the aperture and is, therefore, a linear function of particle volume. The output of the main amplifier is fed to an oscilloscope for pulse shape monitoring and to a multichannel pulse-height analyzer (20) which accumulates the pulse-height distribution which, in turn, represents the particle volume distribution.

At the conclusion of a run, the volume distribution is stored in the memory of the multichannel analyzer. These data may be read out on a printed tape giving the number of pulses recorded in each channel or may be automatically plotted, giving a distribution as shown in Fig. 1. This is the volume distribution of bone marrow cells from the tibia of a CBA mouse. The horizontal axis is divided into 100 increments or channels and corresponds to particle volume in cubic microns. The vertical axis is, on a linear scale, the percent of to-

Fig. 1. Volume distribution of marrow cells obtained from the tibia of a normal CBA mouse. Each point represents one channel of a multichannel analyzer. Projection of a point on the abscissa is proportional to electronic pulse-height and, therefore, to particle volume. In this example, each channel represents a $6 \mu^3$ volume increment. The number of particles (pulses) falling within this increment is represented by projection of the data point on the ordinate.



tal cells per volume increment or channel. Although this multichannel analyzer has a 400-channel capability, only 100 were normally used; thus, each point in Fig. 1 represents a single channel.

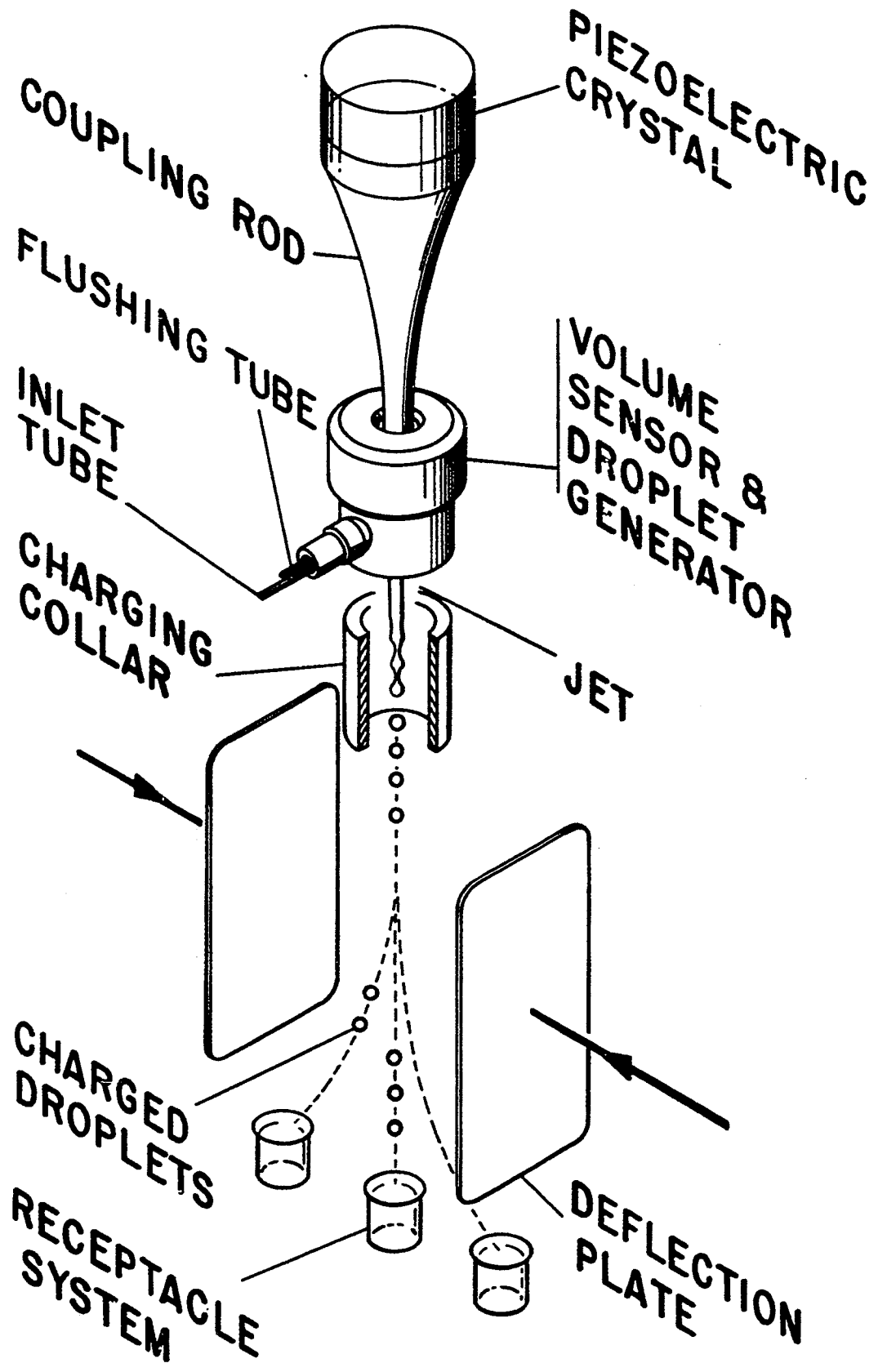
2. Electronic Sorting of Cells According to Difference in Volume

a. Operation and Construction

The cell separator has been briefly described elsewhere (11). Presented here is a detailed description of the operation, construction, and electronics system of an advanced version of the device.

Separation of an individual particle from a suspension of heterogeneous particles is obtained by sensing the volume of every particle, isolating each in a single liquid droplet, and causing deflection of the droplet containing the particle desired. Figure 2 illustrates this scheme. Particles suspended in a conductive liquid enter the volume sensor and droplet generator through an inlet tube. Ultra-sonic vibrations produced by a piezoelectric crystal are transmitted to the particle suspension by a coupling rod. The resulting disturbances on the liquid jet cause droplet formation, leading to isolation of the suspended particles. Several adjacent droplets, one of which contains the desired particle, are electronically charged as they detach within the charging collar. The droplet stream continues on into a constant electric field developed between two deflection plates, wherein the charged droplets are deflected, according to the polarity and magnitude of their charge, and caught in a suitable receptacle [commonly a 10-cc beaker (21)]. This method of droplet formation, charging, and deflection is a modification of that developed by R. G. Sweet as an ink-writing oscillograph. (22).

Fig. 2. Operation and construction of the electronic cell separator.

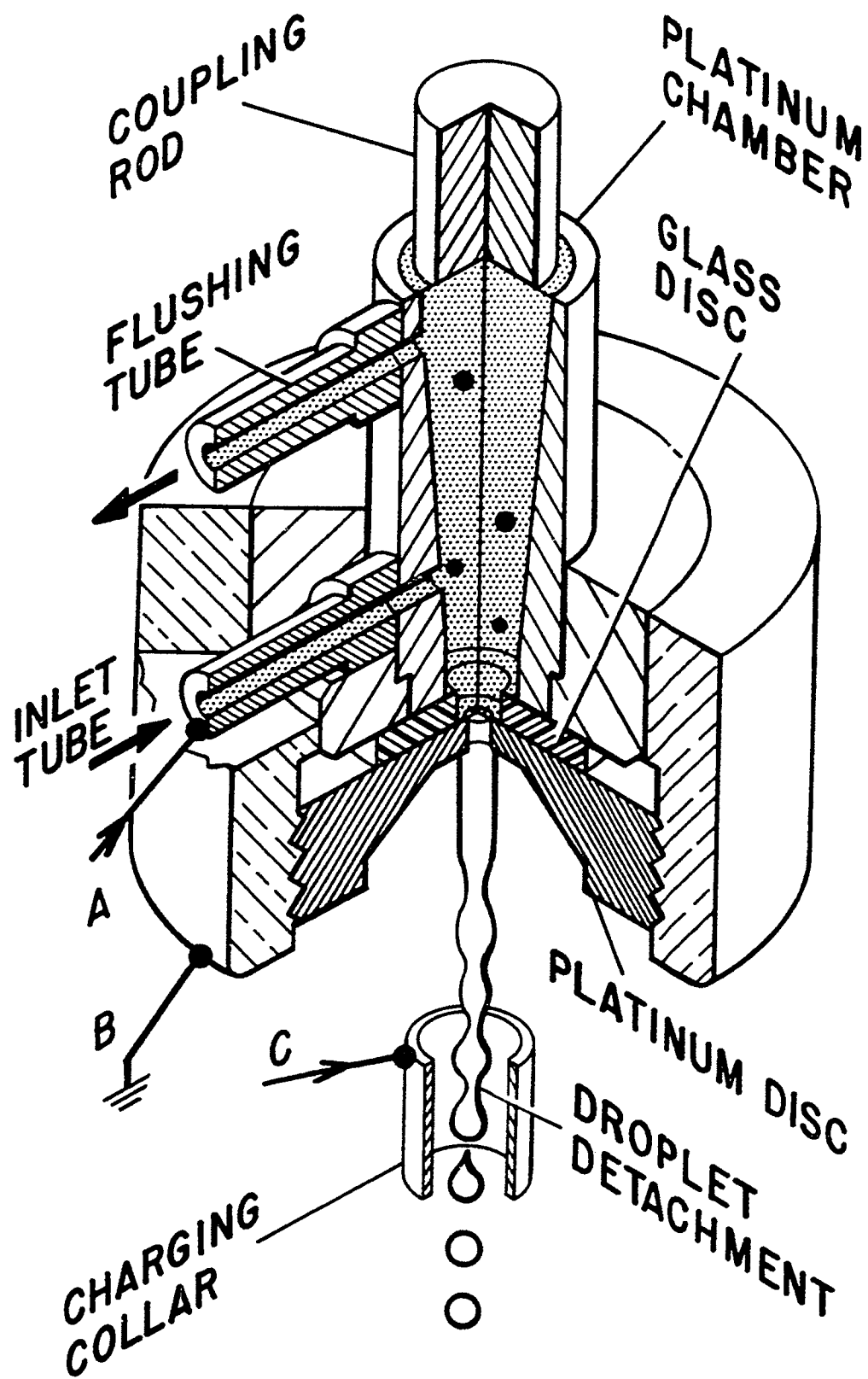


1. Volume Sensor and Droplet Generator

Figure 3 is a cross-sectional illustration of the volume sensor and droplet generator (23). A particle suspension, under a pressure of 2-4 atm, enters through a platinum inlet tube which also serves as an external electrical connection to the platinum chamber. An exhaust or flushing tube is provided to permit removal of air bubbles which, at the beginning, may accumulate on the face of the coupling rod, preventing transfer of acoustic energy. This coupling rod, constructed of plastic and catenoidal in shape, serves as an acoustic transformer, increasing displacement of the rod end in contact with the suspension. Two rubber O-rings (not shown) isolate the plastic coupling rod from the generator and its associated electronic cabling. Because of a favorable acoustic impedance match, energy is efficiently transmitted from the rod to the cell suspension. The interior shape of the chamber serves to concentrate this acoustic energy in the vicinity of the orifice discs.

Externally closing the flushing tube causes the cell suspension to pass through a glass orifice disc and a platinum orifice disc to emerge as a liquid jet. To facilitate illustration, the diameters of these openings have been greatly exaggerated; a typical diameter is 45 μ . The glass disc (serving as a volume sensor) and the platinum disc (serving as an electrode) are joined with an epoxy adhesive and may be removed as a unit by unscrewing. This feature facilitates cleaning and allows selection of a disc assembly suited to the particles being processed. The droplet generator and all associated tubing, electronic cables, etc., are constructed of materials able to withstand sterilization by autoclave.

Fig. 3. Simplified cross-sectional illustration of the volume sensor and droplet generator.



Although it does occur, plugging of the apertures is not a serious problem. Before admission to the droplet generator, the particle suspension passes through a go no-go filter constructed of parallel, fused, glass capillary tubes (24). A commonly used filter has individual bore diameters of $30 \pm 3 \mu$, thus passing particles of less than 27μ and retaining those greater than 33μ . Should it lodge in the aperture, a particle may often be removed by closing the inlet tube and opening the flushing tube to a vacuum, causing air to flow in through the apertures.

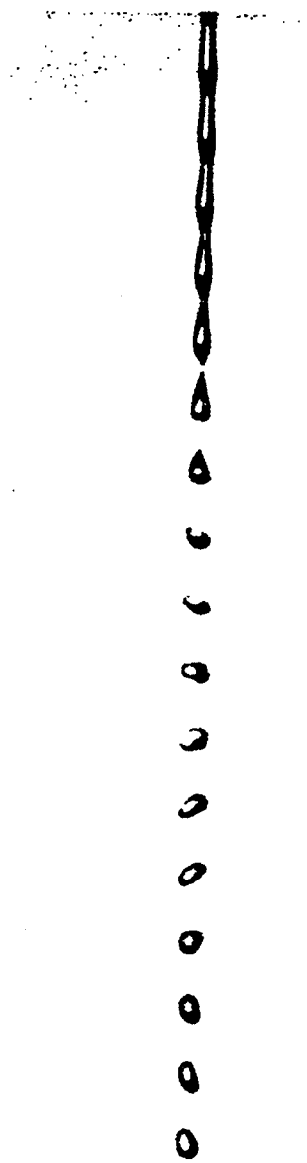
Particle volume is measured using the Coulter principle, as described in the preceding section. A direct constant-current supply is connected between points A and B (Fig. 3). Current flows from the platinum chamber, through the column of conducting liquid confined within the glass disc to the platinum disc, and thence to point B. This glass orifice is approximately 45μ in diameter and 500μ in length; particle transmit time through the aperture is about $50 \mu\text{sec}$.

2. Droplet Formation and Charging

Droplet formation is a result of rapid pressure fluctuations superimposed upon the ambient pressure. These fluctuations in pressure cause small variations in the velocity of the emerging jet, resulting in bunching of the liquid column. Surface tension causes these disturbances to grow until the column is pinched into droplets of very uniform volume and spacing. The rate of droplet formation is equal to the frequency of oscillation of the piezoelectric crystal. Figure 4a shows the emerging liquid jet breaking into approximately

Fig. 4. Liquid droplet formation and deflection (formation rate 70,000/sec, jet diameter approximately 40 μ , and jet velocity about 10 m/sec). The stable droplet diameter is approximately 90 μ^3 , and each represents about 4×10^{-7} ml of liquid.

A



B



70,000 droplets/sec. Jet diameter is about 40μ , and its velocity is about 10 m/sec. When first formed, the droplets are not spherical but oscillate about the spherical shape which they quickly assume, as shown in Fig. 4b; this photograph was taken about 3 cm beyond emergence and shows a group of 7 charged droplets beginning to undergo deflection. Droplets are spaced at 14- μ sec intervals, and each represents about 4×10^{-7} ml of liquid. The stable droplet diameter is approximately 90μ . During separation, one of this group of 7 will contain the cell of interest; the other 6 have a high probability of containing no cells, for reasons which will be explained.

As shown in Fig. 3, droplets are charged by applying a pulsed electrical potential between the charging collar C and point B, which is in electrical contact with the liquid column as it emerges from the platinum orifice disc. Electric current flows until the coaxial capacitor, comprised of the liquid column and the collar, is charged. Detaching droplets carry a charge proportional to the applied voltage; the number charged is determined by the time duration of the charging pulse. The magnitude of these pulses can be varied to assure that the deflected droplets will be adequately spaced from the uncharged droplet stream. In normal operation, two distinct volume classes are simultaneously separated. A positive pulse is applied to droplets containing particles of one class, causing their deflection to one side, and a negative pulse is applied to droplets carrying particles of the second class, causing their deflection to the other side of the main droplet stream.

3. Separation and Timing Considerations

The sequence of events leading to separation is as follows. As a particle enters the glass orifice disc, an electronic pulse -- the magnitude of which indicates particle volume -- is developed between points A and B. If the particle is within a volume range chosen for separation, the electronic system will apply a charging pulse, causing deflection of the drop containing the particle into the proper receptacle. This charging pulse must be delayed a time, typically 250 μ sec, adequate to allow the particle to move from the sensing aperture to the region of droplet detachment. At the conclusion of this delay, the charging pulse is applied and maintained for perhaps 100 μ sec. Assuming a formation rate of 70,000 droplets/sec, 7 droplets will form during this time. One of these 7 will contain the particle of interest. The charged droplets pass through the electric field and are deflected into the proper vessel, completing separation.

The necessity for charging several droplets arises from the uncertainty in transit time of a particle from the sensing disc to the point of droplet formation. Laminar flow through the orifices is essential as liquid turbulence, with its accompanying disturbances, causes random disintegration of the emerging jet. Hydrodynamic drag on the liquid passing through the apertures tends to establish a stable, parabolic, velocity profile, consequently a particle near the wall moves more slowly than one on the axis. Depending upon liquid pressure, aperture diameter, length of the liquid jet, and other factors, the average transit time is approximately 250 μ sec with perhaps 85% of the particles arriving within ± 50 μ sec of this average.

Thus, a charge-pulse duration of 100 μ sec gives an 85% probability of "catching" the particle. If the desired particle is not caught, the separated droplets will probably contain no particles and consequently will not lessen the purity of the separated fraction. These figures are strongly dependent on details of platinum orifice design -- currently in a state of change. Once the liquid stream has emerged, the fluid velocity across the jet is constant, and no further time errors of this type accumulate.

Another less important factor contributing to the timing uncertainty is variation in length of the jet due to disturbances caused by electrolysis of water with evolution of H_2 bubbles at the platinum disc. This factor, which requires that the sensing aperture current be limited to the range 50-200 μ A, produces a time error of perhaps ± 10 μ sec.

In the earlier models, dilution of the particle suspension made unlikely the co-occurrence of 2 particles in a group of 7 droplets. For example, assume that a quantity of suspension containing 1500 particles passes through in 1 sec; this quantity of liquid is divided into 70,000 droplets, giving 1 particle/47 droplets. The probability of finding 2 or more particles in a group of 7 adjacent drops is less than 2%. In order to process particles at a higher rate, the current model incorporates an electronic anticoincidence circuit which senses and remembers the time interval between passage of particles through the aperture. Separation is allowed only if no particle has entered the aperture within an adjustable time interval of perhaps 80 μ sec preceding and 80 μ sec following the particle to be separated.

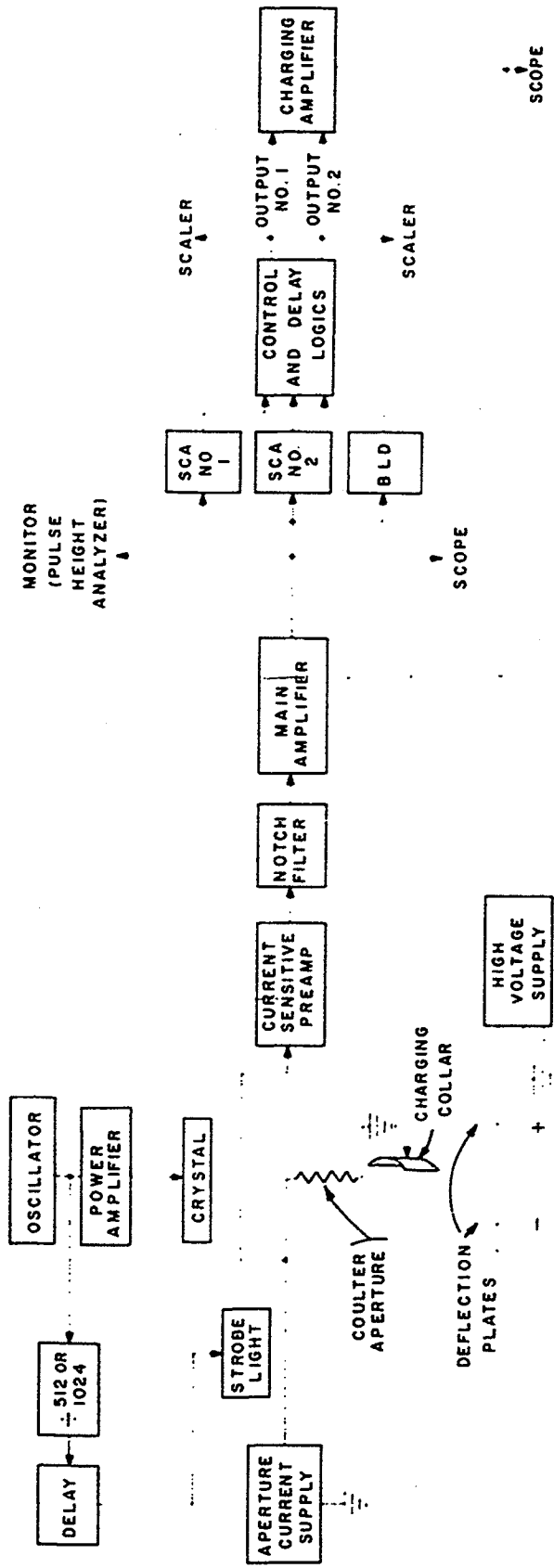
b. Electronics

The block diagram of Fig. 5 will be used in the following description of the system electronics.

1. Droplet Production

Cyclic pressure variations developed in the suspension by action of the piezoelectric crystal lead to droplet production. This crystal is excited by a sinusoidal signal provided by an oscillator (25) and a power amplifier (26). The frequency at which most stable droplet formation is obtained is primarily a function of crystal resonance, jet diameter, and jet velocity. With most aperture disc assemblies, there are several frequency ranges available at which droplet formation is suitable. At resonance, crystal impedance is approximately 1000Ω . The voltage delivered by the amplifier is typically less than 10 V rms, corresponding to less than 100 mW of power. Observation of droplet formation is highly desirable and is achieved using a long working-distance microscope ($\times 30$ magnification) and a stroboscopic light (27). Because of the low firing rate of this light, a dividing circuit is used to provide 1 output pulse per 512, or 1024 cycles of the sinusoidal crystal-driving signal; this output pulse fires the light, making droplet formation appear stationary. The droplet photographs of Fig. 4 were obtained using this scheme. A delay, variable over 1 cycle, can be inserted between divider and strobe light, allowing observation of any part of the droplet formation cycle.

Fig. 5. Block diagram of the electronics system.



2. Droplet Deflection

Two 0-10 kV high-voltage supplies establish the fixed electric field between the deflection plates. These are divided and referenced to ground, providing 0-10 kV positive to one plate and 0-10 kV negative to the other. In operation, the voltage difference between plates is adjusted to approximately 12 kV.

3. Volume Sensing

Measurement of cell volume is obtained using the Coulter principle and the aperture current supply, preamplifier, amplifier, and multichannel analyzer described in the preceding section. Ultrasonic vibrations produced by the piezoelectric crystal introduce into the volume-sensing circuit electronic noise of the crystal-driving frequency. This noise is removed by an active, tuneable, bridged-T notch filter (28) inserted between the preamplifier and main amplifier. The output of the main amplifier is fed to an oscilloscope for pulse shape monitoring and to a multichannel pulse-height analyzer, which accumulates the particle volume distribution. Additionally, the output goes to 2 single-channel analyzers (SCA's) and to a base-line discriminator (BLD).

4. Particle Detection and Selection

The BLD serves two functions: first, to detect the presence of a particle within the aperture, and second, to provide a zero time or fiducial mark from which several logic functions will be timed. Selection of volume pulses representing particles to be separated is

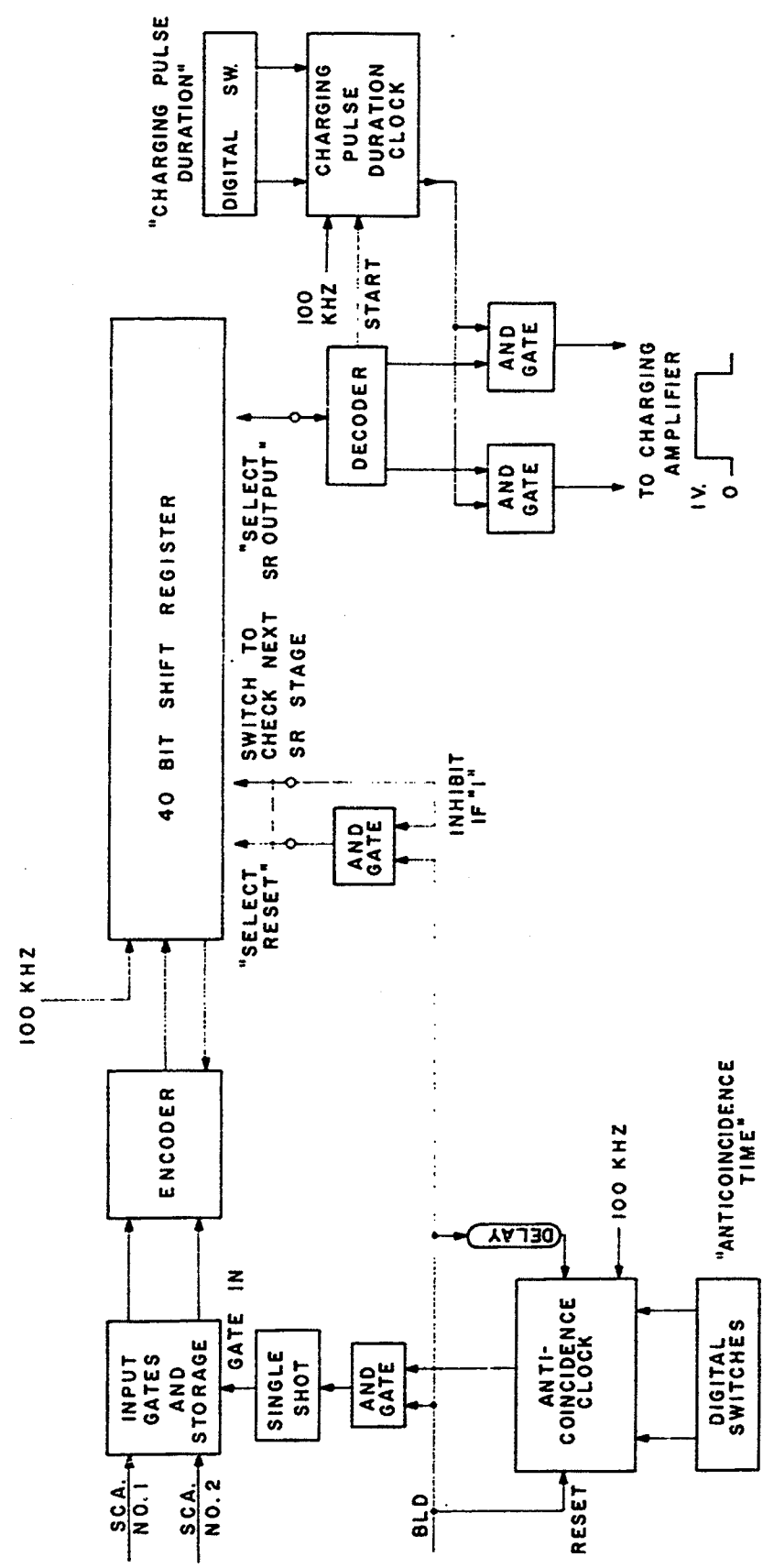
the function of the SCA's. Each SCA consists of an adjustable lower- and upper-level pulse-height discriminator. A volume pulse falling within these limits produces an output pulse which passes into the control and delay logic. Use of 2 SCA's permits simultaneous separation of 2 volume ranges from the sample.

5. Pulse Control and Delay

Several functions are performed by the control and delay logics [Fig. 6 (29)]. This system inserts a selectable time delay between occurrence of a SCA output pulse and initiation of a droplet charging pulse; it also specifies the duration and, according to which SCA was triggered, polarity of this charging pulse. Also incorporated is an anticoincidence circuit which assures that only the particle desired will be found within a group of charged and deflected droplets.

Delay of the charging pulse is obtained as follows. An output pulse from a SCA passes through an input gate into temporary storage, from which a coded 2-bit word is inserted into a 40-bit shift register (SR). A pulse from SCA No. 1 is encoded as 01 and from SCA No. 2 as 11. Information within the SR is transferred along at a 100-kHz rate; consequently, each position represents a 10- μ sec delay. By selecting the position at which information is removed from the SR, delays of up to 400 μ sec are available. The SR output is transferred to a decoder, where 01 activates one output gate and 11 the other. The charge pulse duration clock is initiated simultaneously, providing a 1-V output pulse of a duration adjustable in 10- μ sec steps from 10-990 μ sec. Used in this way, a SR minimizes system dead time by allowing a second pulse (particle) to be processed while a previous pulse

Fig. 6. Pulse control and delay logics.



is being delayed.

As explained earlier, hydrodynamic drag within the apertures introduces an uncertainty in particle position, requiring that several adjacent droplets be charged in order to catch the one carrying the particle. At low concentrations, the probability of finding more than one particle in a group of deflected droplets is small; however, at higher concentrations -- desirable because of the correspondingly greater rates of separation -- this probability increases, leading to impure separated fractions. The anticoincidence circuit allows separation of a particle only if it is sufficiently spaced from preceding and following particles so that it alone will be found in the group of deflected droplets. This is accomplished by addition of one timer ("anticoincidence clock") and use of the SR as a second timer. The anticoincidence clock is set to run a time adequate to ensure isolation of a desired particle from the preceding particle. Each BLD pulse, representing a particle in the aperture, resets and starts this timer; while it is running, the "AND" gate is disabled and the input gates remain closed, preventing insertion of data into the SR. The SR is used as a second timer by tapping (see "select reset") into a position corresponding to the selected anticoincidence time. Each BLD pulse causes erasure of all data lying between the first SR stage and the tapped position, thus ensuring that a particle will not be separated unless it is adequately spaced from the following particle. SCA No. 2 code word 11 might be converted into SCA No. 1 code word 01 by erasing the trailing 1; this is avoided by allowing reset only if the next higher SR position contains a 0.

To aid explanation, consider an example in which the anticoincidence time is chosen to be 80 μ sec (i.e., the anticoincidence clock runs 80 μ sec, and the reset switch corresponds to the 80- μ sec position of the SR). A particle within the desired volume range enters the aperture. Because the clock is timed out, the BLD pulse opens the input gates, resets and starts the clock, and resets the early stages of the SR. After all of this has occurred, the SCA output pulse arrives and is passed into temporary storage, from which it is encoded into the SR and transferred along at a 100-kHz rate. After a total of 60 μ sec has passed, a second particle enters the aperture, producing a BLD pulse which resets the early positions of the SR and thereby erasing the previously accepted pulse. Because the anticoincidence clock is running, the "AND" gate is disabled and the input gates remain closed, preventing entry of a SCA pulse should it occur. Additionally, the BLD pulse resets and starts the clock. Consequently, in order for a particle to be separated, it must be spaced at least 80 μ sec from the preceding and following particles. Obviously, this scheme requires that each particle passing through the aperture produce a BLD pulse which, in turn, requires that two particles be spaced at least one aperture transit time apart -- about 50 μ sec. The anticoincidence time is adjustable from 80-200 μ sec.

6. Droplet Charging

The charging amplifier (30) of Fig. 5 receives from the logic chassis a digital signal of predetermined duration. This charging circuit must provide a stable analog output pulse of preselected amplitude and of a positive or negative polarity, depending on which

of the two input lines from the logics is energized. The charging pulse produced is "square," rising in 1.5 μ sec to a stable level which may be adjusted between 20 and 100 V. Two scalers count the output pulses from the logics to give an estimate of the number of particles separated.

B. Biological Methods and Materials

1. Volume Analysis of Human Leucocytes in Peripheral Blood

a. Concentration of Leucocytes

Because leucocytes occur infrequently (1 in 500) among the cells of whole blood, it is necessary to minimize interference by erythrocytes. Concentration is achieved using a modification of the procedure described by Herbeuval et al. (31) in which saponin is used to lyse the erythrocytes. The starting material is 5 ml of heparinized whole blood. Herbeuval's procedure is modified by first spinning the cells down and then washing them in phosphate-buffered saline. After lysis, the cells are layered over 1 ml of the donor's plasma and centrifuged through, thereby minimizing further saponin action. Finally, the pellet is resuspended and diluted with buffered saline to a concentration suitable for analysis and separation. This method produces a suspension stable in cell volume for about 1 hour. Lymphocyte recovery is quantitative, but some loss of other cell types occurs.

b. Microscopic Examination of Separated Cells

In order to examine cells obtained by separation, it was necessary to develop a technique to remove quantitatively as few as 10^4

cells from very dilute suspensions and to deposit them on a coverslip. A special centrifuge tube was constructed of Teflon with a conically shaped cavity tapering to a circular area 3.6 mm in diameter. Coverslips are mounted against this opening to receive the centrifuged cells. After deposition, cells are fixed and stained with Wright's stain.

2. Cell Volume in Mouse Hemopoiesis

a. Preparation of Cell Suspensions

Bone marrow cell suspensions are obtained by a modification of the method of McCulloch and Till (32). Female CBA mice obtained from Jackson Laboratories are killed by cervical dislocation. A tibia is removed and cleaned of muscle, and the epiphyseal cap is detached. The distal end of the bone is severed using scissors. Marrow is removed by inserting a 26-gauge needle (20-gauge for femur) in the severed end and aspirating through the shaft with 5 ml of diluent IIa (defined on page 33). The resulting cell clumps are dispersed by repeated, vigorous pipetting of the suspension in a 5-ml pipette. Treated in this way, the average tibia yields approximately 8×10^6 nucleated cells suspended in 5 ml of medium. Nucleated cell concentration is obtained using a Coulter Counter Model B. Only cells of volume greater than $90 \mu^3$ are counted, giving a value in close agreement with cell count after saponin lysis. Cell suspensions are normally kept in ice until needed.

Spleen cell suspensions are obtained by excising the spleen free of supporting tissue. Two methods of cell dispersal have been tried, but no significant differences were observed. In one method, the

spleen is minced with scissors into small particles. Single-cell dispersal is achieved by repeated, vigorous pipetting in a 5-ml pipette. Before counting, the suspension is passed through a No. 500 stainless steel mesh of approximately 30 μ opening diameter. In the alternate method, the spleen is placed in a petri dish with 0.1 ml of versene solution (2×10^{-3} M EDTA, 5×10^{-4} M PO_4 , pH 7.0) and gently massaged to break the cells free of supporting tissue. Single-cell dispersion is again obtained by vigorous pipetting.

b. Titration of CFU

The method of CFU titration used is a modification of that developed by Till and McCulloch (33). Eight- to 12-week-old CBA mice obtained from Jackson Laboratories were used in these experiments. The number of mice used per experiment varied; however, 2 or more were used for each CFU titration. Most mice are irradiated with a single dose of 800 rads of 230-kV X rays. In some cases, mice received 700 rads delivered whole body followed immediately by 450 rads to the spleen only. No significant difference in endogenous colony formation was observed; however, the latter method gives better survival of young mice. Cell suspensions prepared as described above are injected in a lateral tail vein using a 27-gauge, $\frac{1}{2}$ -in. Huber point, hypodermic needle; normally 0.5 ml or less is injected. Unlimited food and water are allowed. Seven to 10 days after injection the host mice are killed, and their spleens are excised, fixed in Bouin's solution, and scored for colonies.

c. Microscopic Examination of Separated Cells

Between 0.1 and 0.3 ml of cell suspension containing 10^4 or more cells in diluent IIa is placed in the special Teflon tube previously described and centrifuged for 5 minutes at 300 g. The supernatant is removed using an absorbent wick of filter paper. The coverslip is removed and air-dried for 10 minutes, fixed for 2 minutes in absolute methanol, and stained with Wright's stain.

d. Differential Counting of Cell Types

A minimum of 200 cells per sample are counted and classified according to the criteria of Puck (34).

III. RESULTS

A. Volume Analysis and Particle Separation

1. Polystyrene Spheres

A fractionation of polystyrene spheres is shown in Fig. 7. These volume distributions were obtained using a modification of the Coulter Counter and a current supply, preamplifier, amplifier, and multichannel analyzer as described earlier. A mixture of polystyrene spheres (18), ranging in diameter from 6-14 μ , gave the curve of closed circles. The separator was adjusted to remove simultaneously 2 distinct volume ranges. These fractions were collected in beakers, and their volume distributions were obtained giving the 2 remaining curves. Fraction 1 had a modal volume of approximately 160 μ^3 and fraction 2 a modal volume of approximately 250 μ^3 . This volume difference corresponds to a diameter difference of about 1 μ .

2. Mixture of Human and Chicken Erythrocytes

Figure 3 illustrates application of the device to biological cells. It was the objective of this experiment, performed in collaboration with Dr. Wright Langhem, to test the ability of the separator to isolate cleanly 2 distinct classes of cells of different volume. Human and chicken erythrocytes, the latter being nucleated and larger, were mixed and gave the volume distribution shown. The separator was adjusted to remove cells from the indicated volume ranges, which are widely spaced to avoid the ambiguous region in which the 2 populations overlap. The isolated cells, along with the input sample, were deposited on microscope coverslips, stained, and photographed as shown

Fig. 7. Fractionation of polystyrene spheres of 6-14 μ diameter.

The modal volume of fraction 1 is $160 \mu^3$ and of fraction 2 is $250 \mu^3$,
corresponding to a diameter difference of about 1μ .

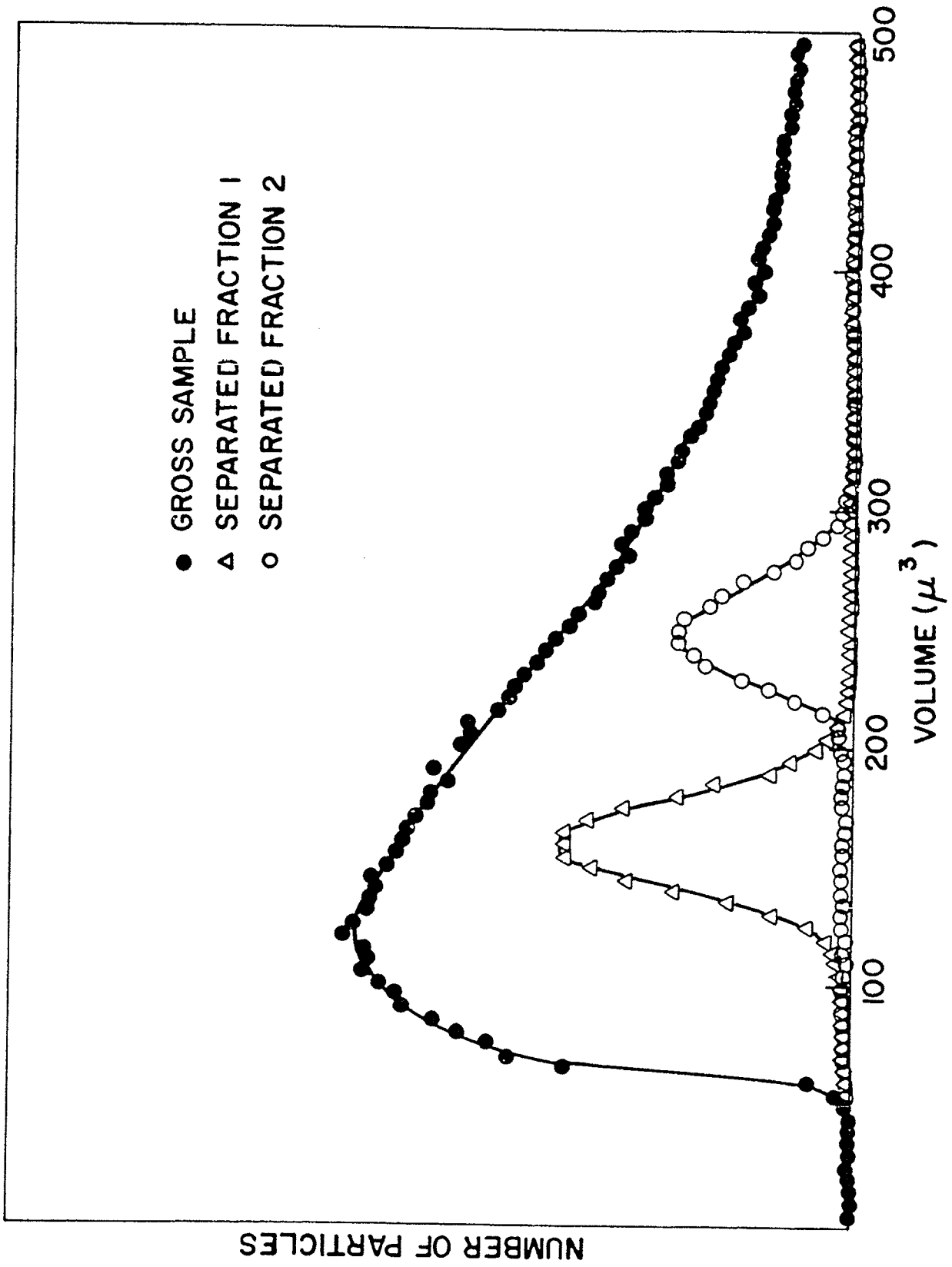


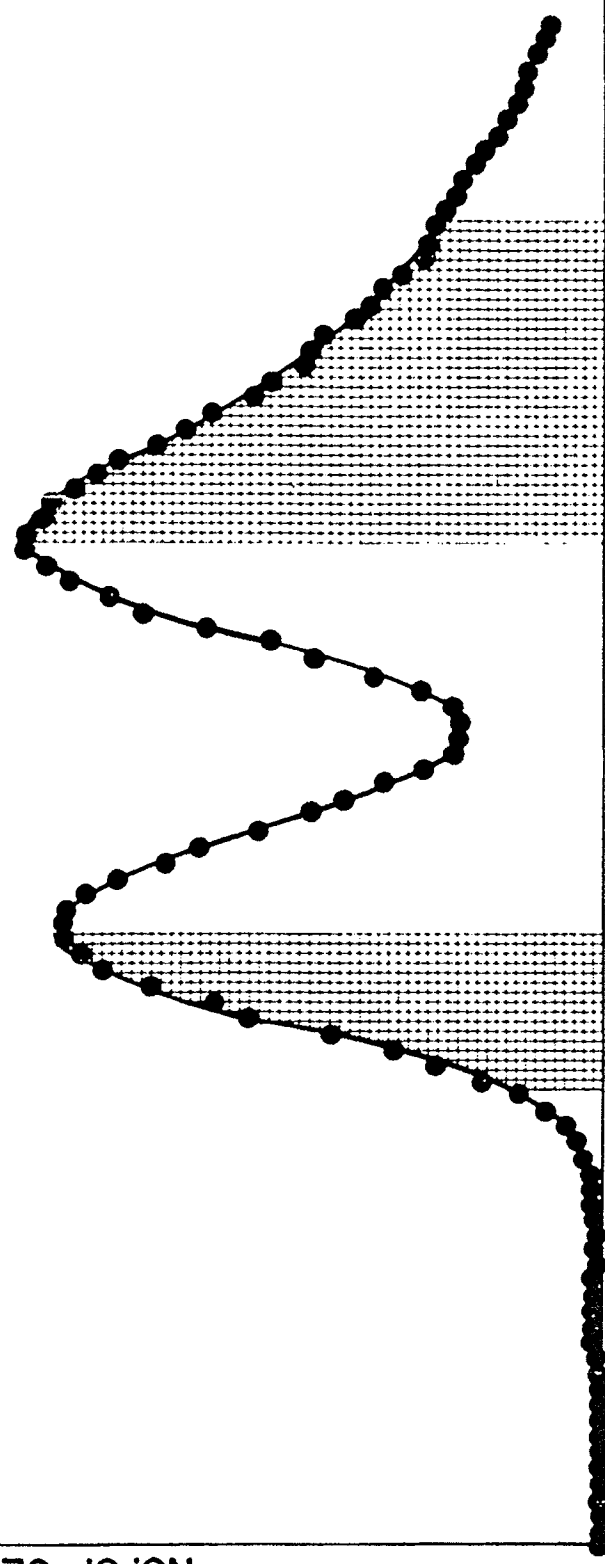
Fig. 8. Volume distribution of a mixture of human and chicken erythrocytes. The peak of smaller volume (modal value approximately $75 \mu^3$) represents erythrocytes from a microcytic individual, and the chicken erythrocytes give the larger peak (modal value approximately $120 \mu^3$). The shaded areas were separated, yielding a fraction of which 95% were chicken cells and a fraction of which 99% were human cells.

MIXTURE OF HUMAN RED BLOOD CELLS
AND CHICKEN RED BLOOD CELLS

● BEFORE SEPARATION

NO. OF CELLS

VOLUME



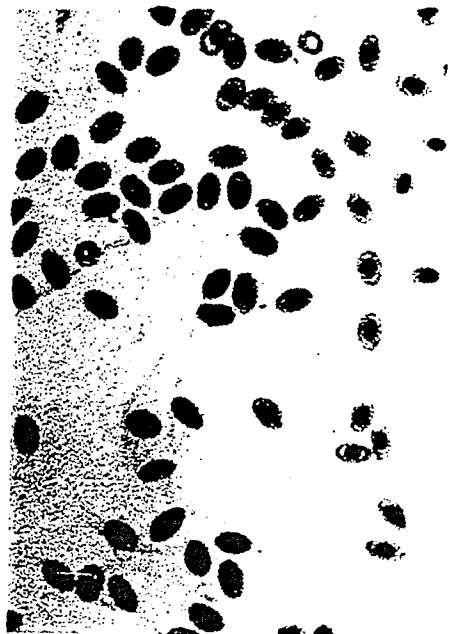
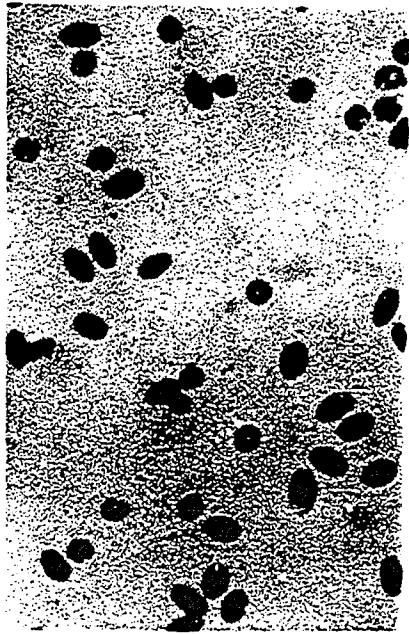
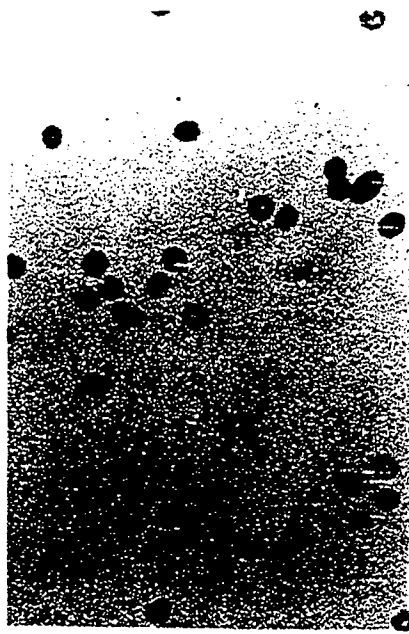
in Fig. 9. Presented from left to right are the mixture, the cells from the small volume fraction, the cells from the large volume fraction, and a table giving the purity obtained from a starting mixture of 60% human cells and 40% chicken cells. The lower purity of the separated chicken cells resulted because 2 small human cells stuck together can produce a particle with the volume of a chicken cell. Separation of this duplex particle results in a lessening of purity. The reverse process, 2 chicken cells being mistaken as a human cell, is not possible.

R. Application to Biological Problems

1. Development of a Volume-Stabilizing Medium

Meaningful use of volume sensing devices requires that cell volume remain constant during the course of analysis. Shifts of cell volume may cause a loss in detail of the distribution and obscure a minor cell population. For many applications of cell separation, the volume distribution of the sample must remain stable for as long as 2 hours. A medium (designated IIa) suitable for the described mouse cells has been developed and consists of physiological saline (9 g NaCl/l. of H₂O) to which is added 2 λ /ml of fetal calf serum and 10 units/ml of heparin (Panhetrin-Abbot Laboratories); the solution is buffered at pH 7.0 with 3×10^{-3} M PO₄. Distribution stability is illustrated in Fig. 10. In this experiment, cells were removed from the tibia of a CBA mouse and dispersed, as described in Methods, in diluent IIa. Volume distributions were obtained immediately (curve of X's), 1 hour later (curve of closed circles), and at 1 hour and 40 minutes (curve of open circles). There has been little, if

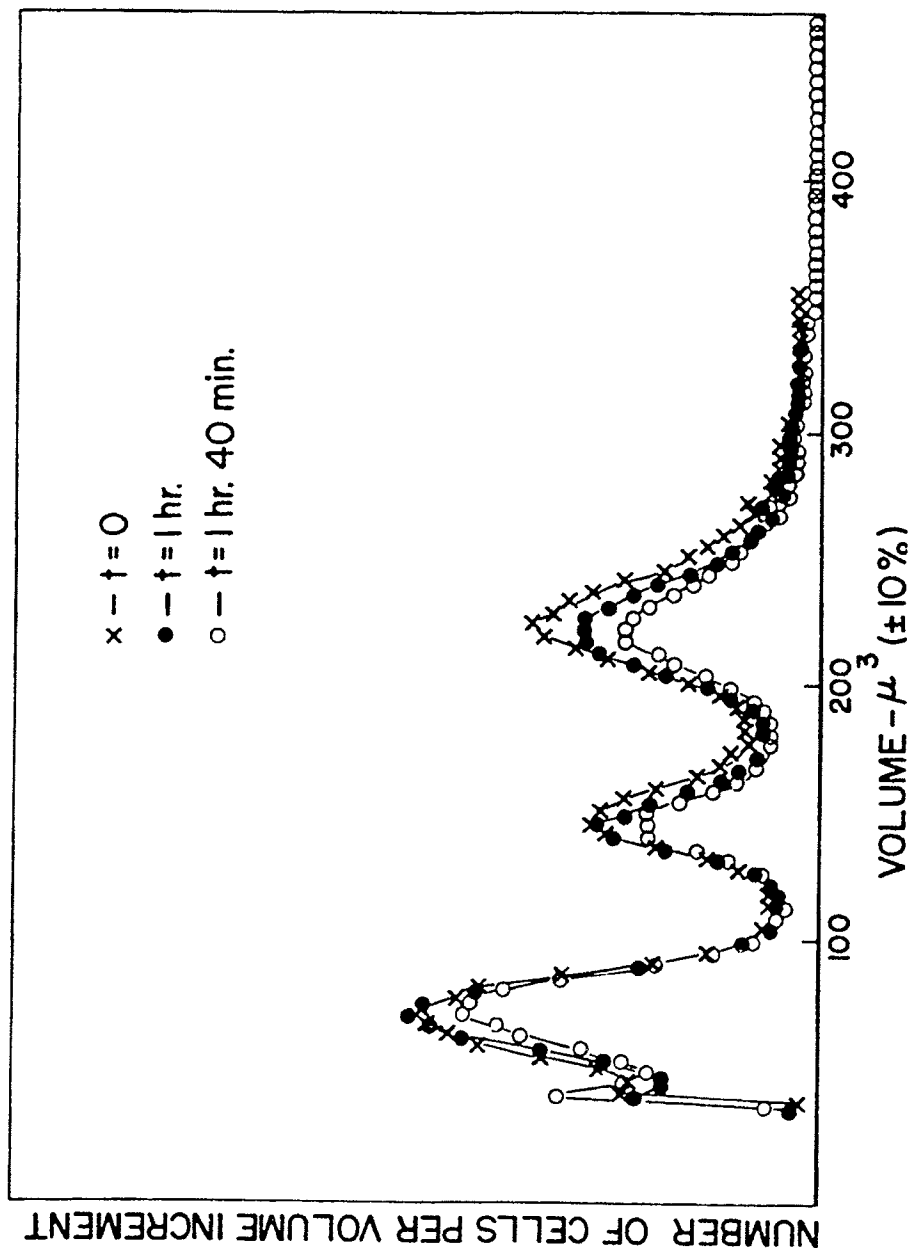
Fig. 9. Photomicrographs of a mixture of human and chicken erythrocytes and of 2 separated fractions, along with a table giving purity of the separated fractions.



SEPARATION OF 60/40 MIXTURE OF
HUMAN AND CHICKEN ERYTHROCYTES

Fraction	Separation Efficiency (percent)
Sep. Human Cells	99
Sep. Chicken Cells	95

Fig. 10. Volume distributions of mouse bone marrow cells at various times after dispersion in a volume-stabilizing medium. The distributions remain stable over a 1 hour and 40-minute period. CFU viability is excellent.



any, displacement of peak modal values. Vertical displacement of the curves reflects the settling or attachment of cells to the glass walls of the counting vessel. Viability of colony-forming cells in this diluent is excellent.

2. Viability of Separated Cells

For many applications of the cell separator, viability of separated cells is of utmost importance. A cell is subjected to ultrasonic energy while in the platinum chamber and traversing the orifice. The amount of power developed by the crystal-driving amplifier is ordinarily less than 100 mW; however, due to the electrical capacitance of the coaxial cable, the low conversion efficiency of a piezoelectric crystal, and the losses associated with transfer of acoustic energy from the crystal to the solution via the coupling rod, the amount of energy delivered to the cell suspension is probably less than 10 mW. The cells are exposed to this treatment for about 1 minute before entering the orifice. During passage through the orifice, the cells experience hydrodynamic shear forces until emergence in the liquid jet. As the droplet containing the cell detaches, it may be charged by applying a nominal 30-V pulse to the charging collar, giving a charge per droplet of about 10^{-12} coulombs. Aerodynamic forces quickly act on droplets deflected away from the main droplet stream to retard their forward motion; consequently, the droplets slow and strike the liquid surface in a receptacle so lightly that observation is difficult. During sensing and separation, the cell is enveloped in a favorable medium which can be adjusted to specific cell requirements.

Studies at the Biomedical Research Group of the Los Alamos Scientific Laboratory using Chinese hamster ovary cells have demonstrated that at least 96% of the cells retain the function of active membrane transport as determined by the trypan blue exclusion test and by the uptake of tritiated thymidine. The growth rate of cells passed through the separator was indistinguishable from that of the control population (i.e., 21 hours).

Using techniques described in the Methods section, 94% of the colony-forming units (CFU's) found in mouse bone marrow retain their ability to produce progeny after passage through the device. As used here, survival is defined as the ratio of the titer (CFU/10⁴ nucleated cells) of the treated sample (passed through the separator) to the titer of an untreated aliquot of the same sample. Within statistical uncertainty of the titration method, this survival is not distinguishable from 100%.

Chinese hamster ovary cells suspended in sterile balanced salt solution were passed through the separator, collected, and plated in 4 ml of McCoy's FC-10 medium. One week later colony counts were made and compared with the counts of an untreated control. Plating efficiency was 85%, illustrating that processed cells are able to proliferate.

3. Volume Analysis of Human Leucocytes in Peripheral Blood

The study of human leucocytes presents a potentially very fruitful area of application of electronic cell analysis. By establishing the normal volume pattern and correlating this pattern with morphological cell type, a reference is obtained to which abnormal con-

ditions may be related. Because of the rapidity of cell analysis (over 50,000/min) and because of the sensitivity of these instruments to small changes in cell volume, early indication of a pathological state might well be possible. A portion of the work described in this section has been published (35). All of this work was done in collaboration with Drs. M. A. Van Dilla and I. U. Boone of the Biomedical Research Group, Los Alamos Scientific Laboratory.

a. Normal Human Leucocytes

The volume distribution of leucocytes, obtained from a normal male subject and processed as described in the Methods section, is shown in Fig. 11. Whole blood, primarily erythrocytes, gives the curve of open circles. The vertical scales of the two distributions are unrelated. The small peak of the leucocyte distribution reflects incomplete lysis of erythrocytes. The leucocytes are larger and show a bimodal distribution. Cells from the indicated areas 1, 2, and 3 were electronically separated, microscopically examined, and photographed (Fig. 12). These photographs were taken at the same magnification ($\times 680$) and clearly show the expected progression in size. Table I compares cells of the separated fractions (divided into 3 classes) and the unseparated sample. The lesser volume leucocyte peak (fraction 1) represents primarily lymphocytes. The central part of the greater volume peak (fraction 2) is mostly polymorphonuclear granulocytes, and the tail (fraction 3) shows a 15-fold enrichment of monocytes.

Fig. 11. Volume distribution of normal human leucocytes. The 3 shaded areas were separated, stained, and photographed. Whole blood gives the curve of open circles and serves to establish a volume reference.

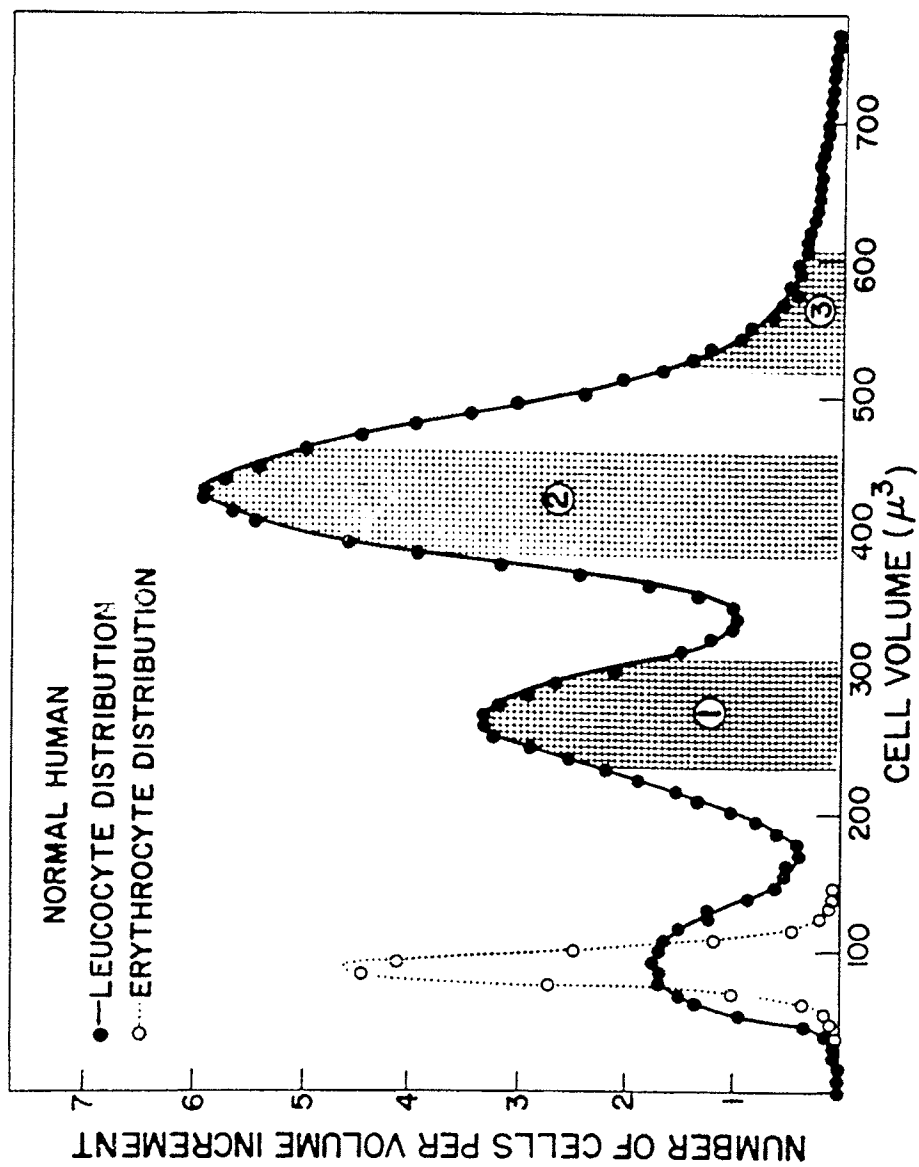
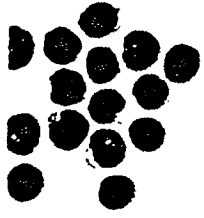


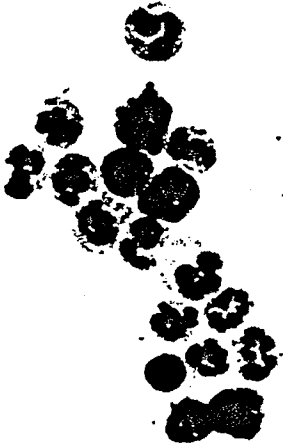
Fig. 12. Photomicrographs of separated fractions 1, 2, and 3 and of the gross mixture. Of the cells in fraction 1, 99% are lymphocytes, of fraction 2, 93% are granulocytes, and of fraction 3, 67% are granulocytes and 30% are monocytes.



1



3



MIXTURE



2



TABLE I
 HUMAN LEUCOCYTE SEPARATION: CELL TYPES PRESENT
 IN THREE AREAS OF THE VOLUME DISTRIBUTION

Volume Separation	Distribution (%)		
	Lymphocytes	Granulocytes	Monocytes
Unseparated	40	58	2
Fraction 1	99	1	0
Fraction 2	5	93	2
Fraction 3	3	67	30

b. Abnormal Human Leucocytes

Figure 13 gives the volume distribution of peripheral leucocytes obtained from a person having infectious mononucleosis. Comparing this with the normal pattern of Fig. 11 illustrates that the abnormal state of this disease is reflected in the leucocyte volume distribution. Four fractions were isolated, as described above, and are shown in Fig. 14. These photographs were taken at x 680 magnification, enlarged x 2.61 and again show a progression in size. The cells obtained from region 1 are small lymphocytes showing somewhat more cytoplasm. Abnormal cells characteristic of infectious mononucleosis appear in region 3. Polymorphonuclear leucocytes, along with abnormal cells are found in region 4.

Figure 15 presents the volume distribution of leucocytes from another individual with infectious mononucleosis. For reference,

Fig. 13. Volume distribution of peripheral leucocytes from a patient having infectious mononucleosis. The 4 shaded and numbered areas were separated, stained, and photographed and are shown in Fig. 14.

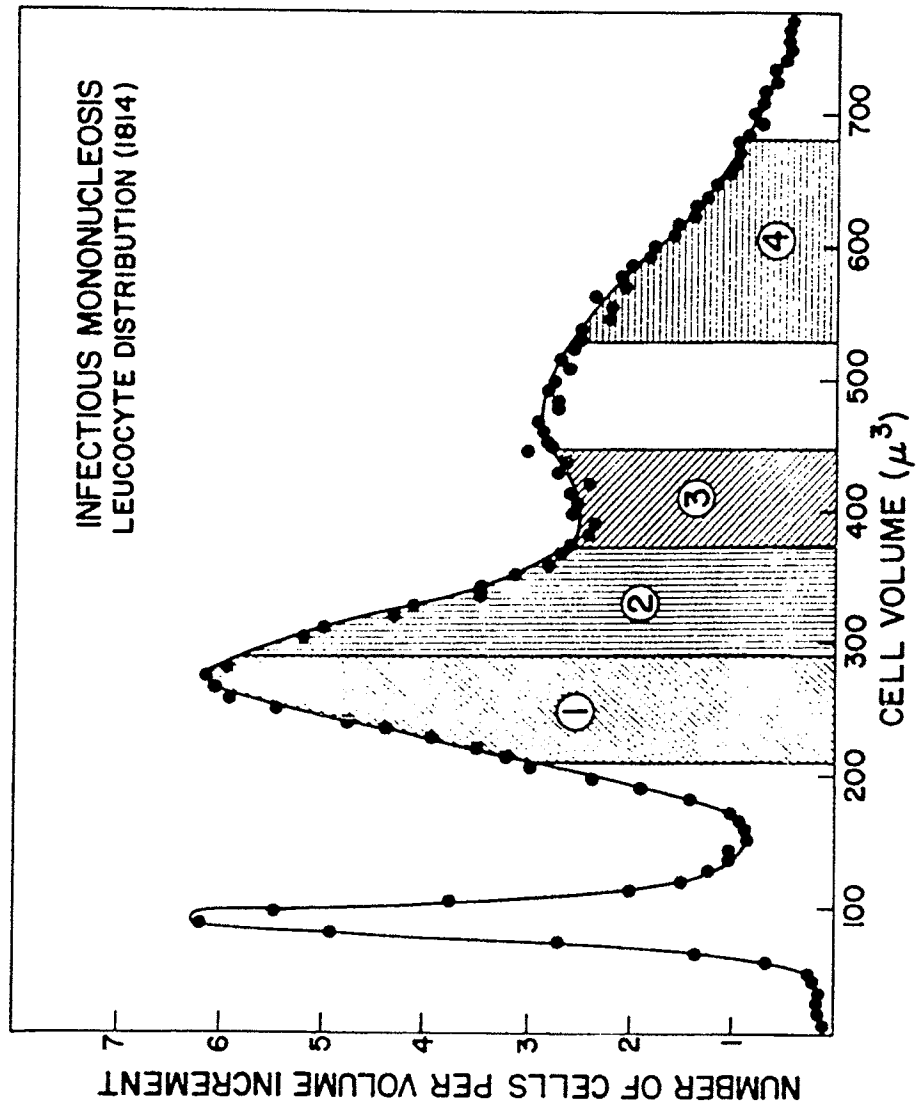
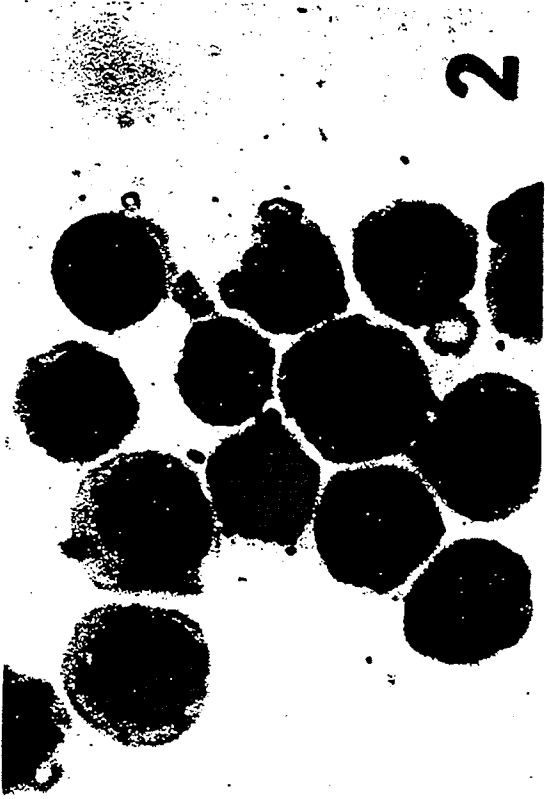


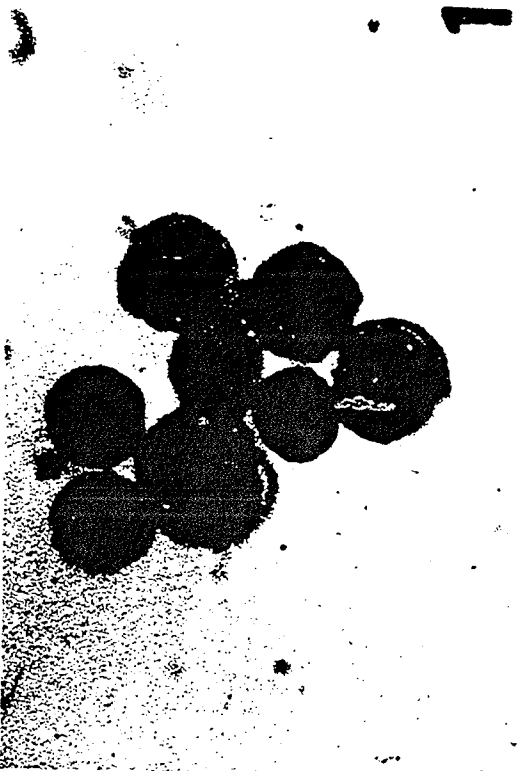
Fig. 14. Cells isolated from peripheral leucocytes of a patient having infectious mononucleosis. These photomicrographs were taken at the same magnification and show a progression in size.



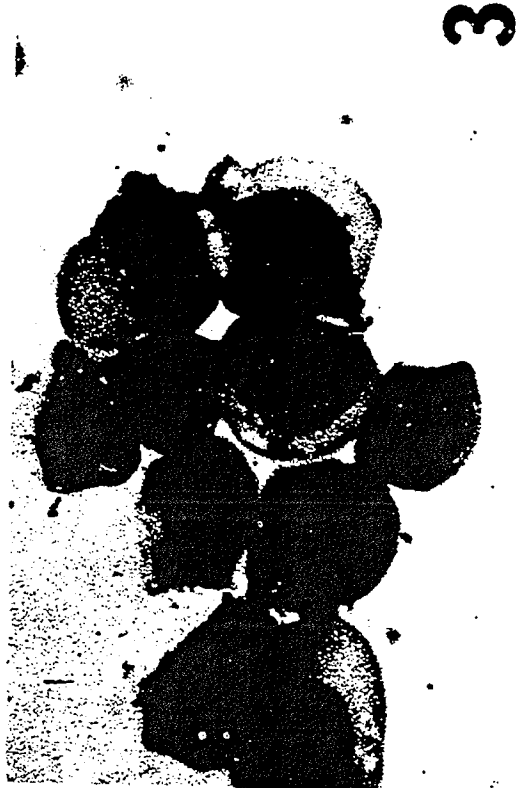
2



4

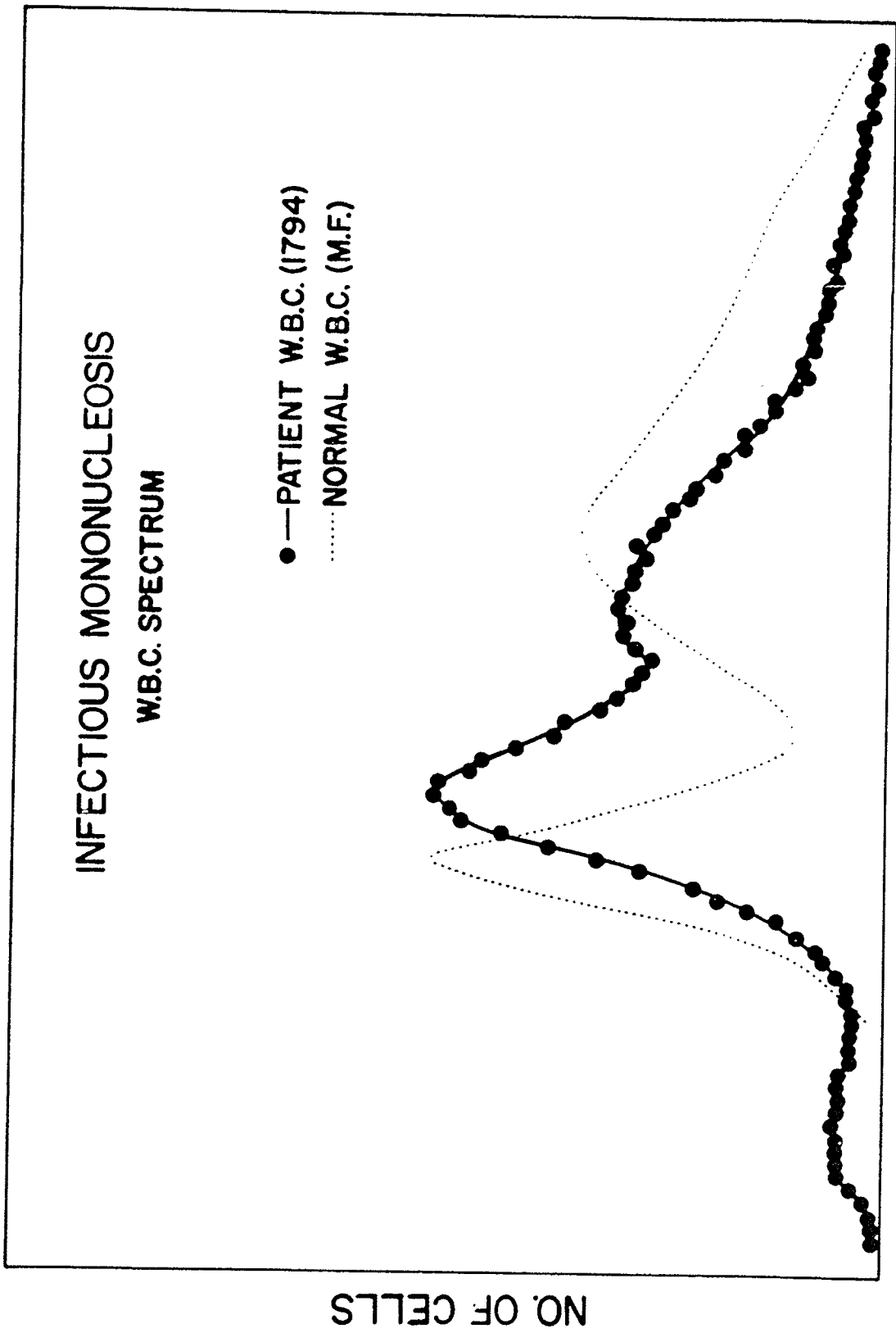


1



3

Fig. 15. Volume distribution of leucocytes in infectious mononucleosis compared with normal leucocytes.



the distribution of normal leucocytes is given as a dotted line. This pattern reflects differences from normal, as did the preceding case. Leucocytes from a case of acute lymphoblastic leukemia compare with the normal distribution as shown in Fig. 16. The great abundance of large lymphocytes is obvious. A freshly diagnosed case of chronic lymphocytic leukemia gives the leucocyte distribution of Fig. 17; this distribution is again quite different from normal.

4. Cell Volume in Mouse Hemopoiesis

a. Volume Analysis of Normal Mouse Bone Marrow and Spleen

A representative volume distribution of bone marrow cells obtained from a CBA mouse is shown in Fig. 18. The curve of closed circles is the distribution of cells isolated, as described earlier, from the tibia of a female CBA mouse. The curve of open circles is the distribution of whole peripheral blood from the same mouse. It can be seen that in region I the bone marrow distribution has 2 modal values, the smaller of which represents mature red blood cells and corresponds to the modal volume of peripheral blood (approximately $60 \mu^3$ in this medium). The larger mode of this region (approximately $82 \mu^3$) is thought to be a result of the abundance of large, immature erythrocytes found in bone marrow. This distribution was selected because of the resolution of these two modes; such detailed structure in region I is not usually apparent unless special effort is taken to disperse the marrow into single cells, as in this example in which the cells were dispersed in a versene-containing medium.

The modal value of the peaks in regions II and III were found to

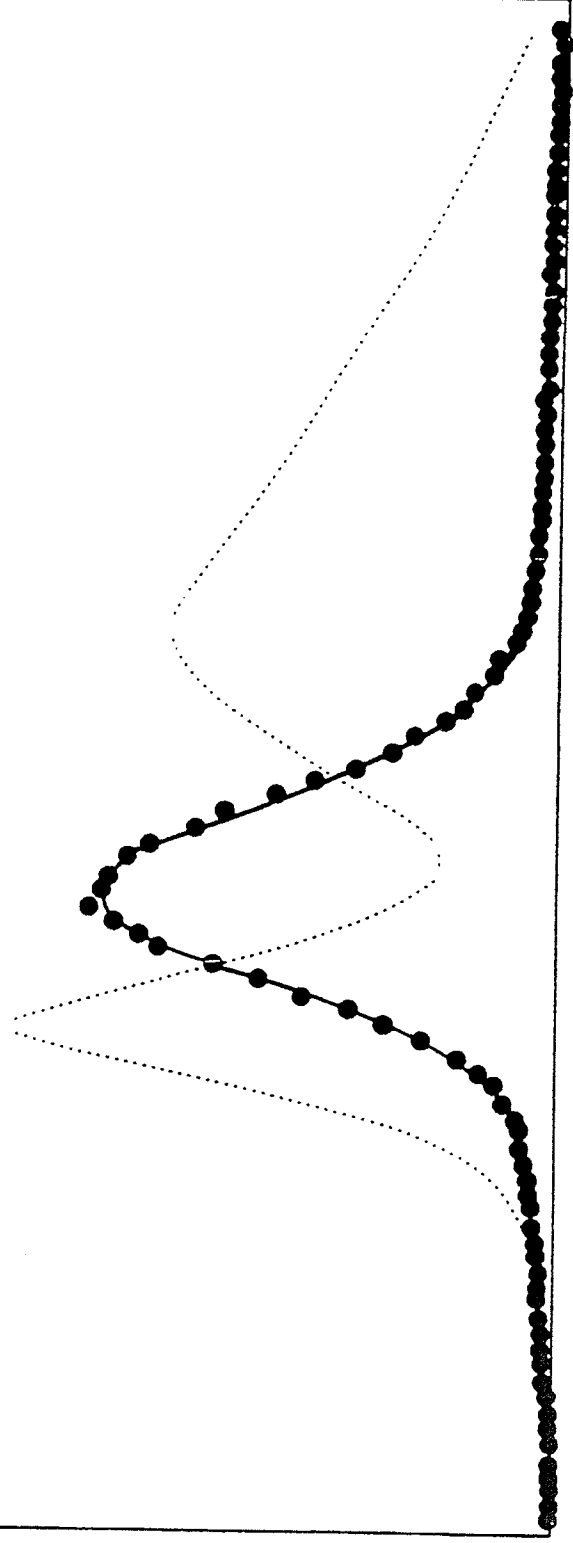
Fig. 16. Volume distributions of leucocytes from peripheral blood of a normal person and a person having acute lymphoblastic leukemia.

ACUTE LYMPHOBLASTIC LEUKEMIA

W.B.C. SPECTRUM

●— PATIENT W.B.C. (I767)
..... NORMAL W.B.C. (M.F.)

NO. OF CELLS



VOLUME

Fig. 17. Volume distributions of leucocytes from the peripheral blood of a normal person and a person having chronic lymphocytic leukemia.

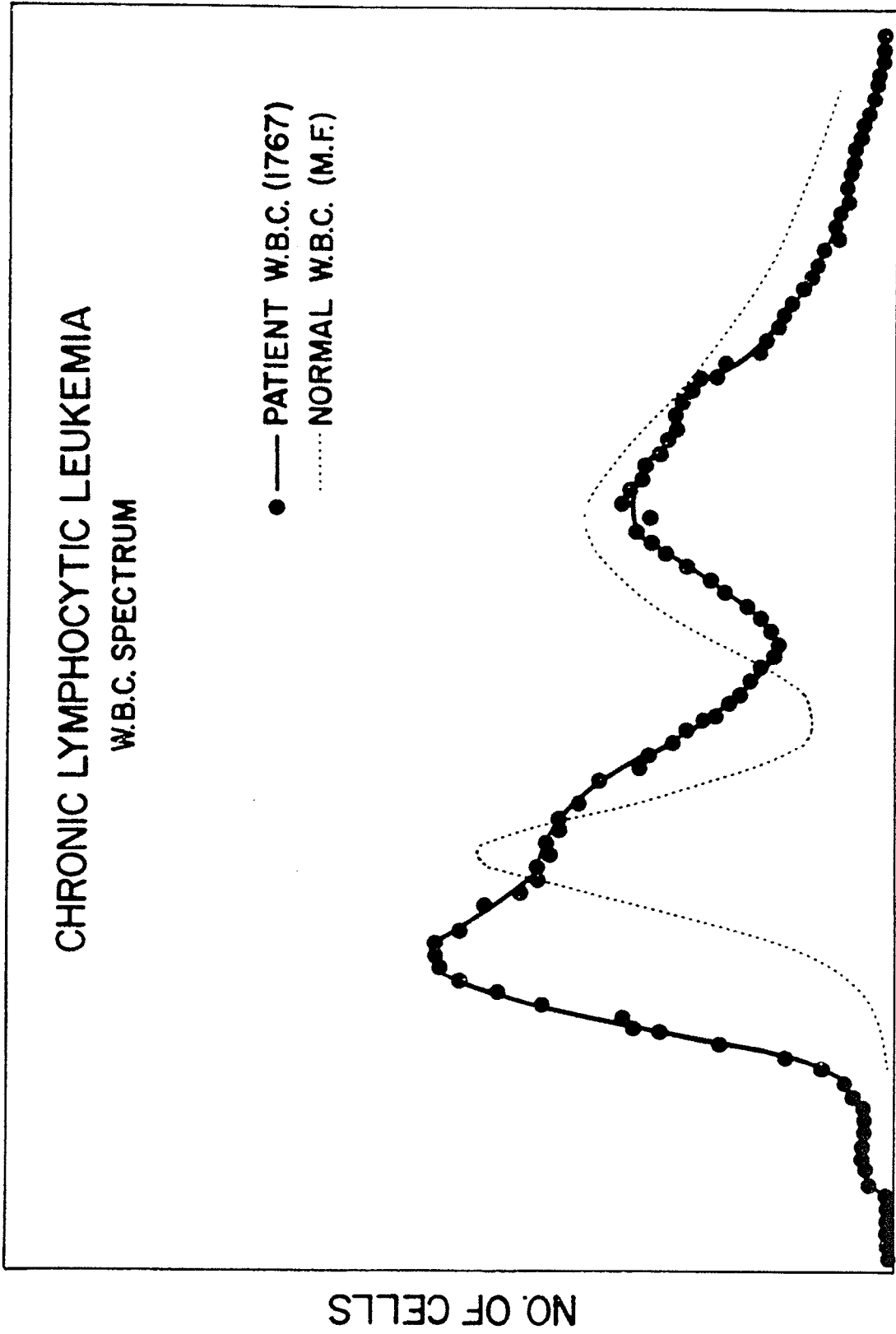
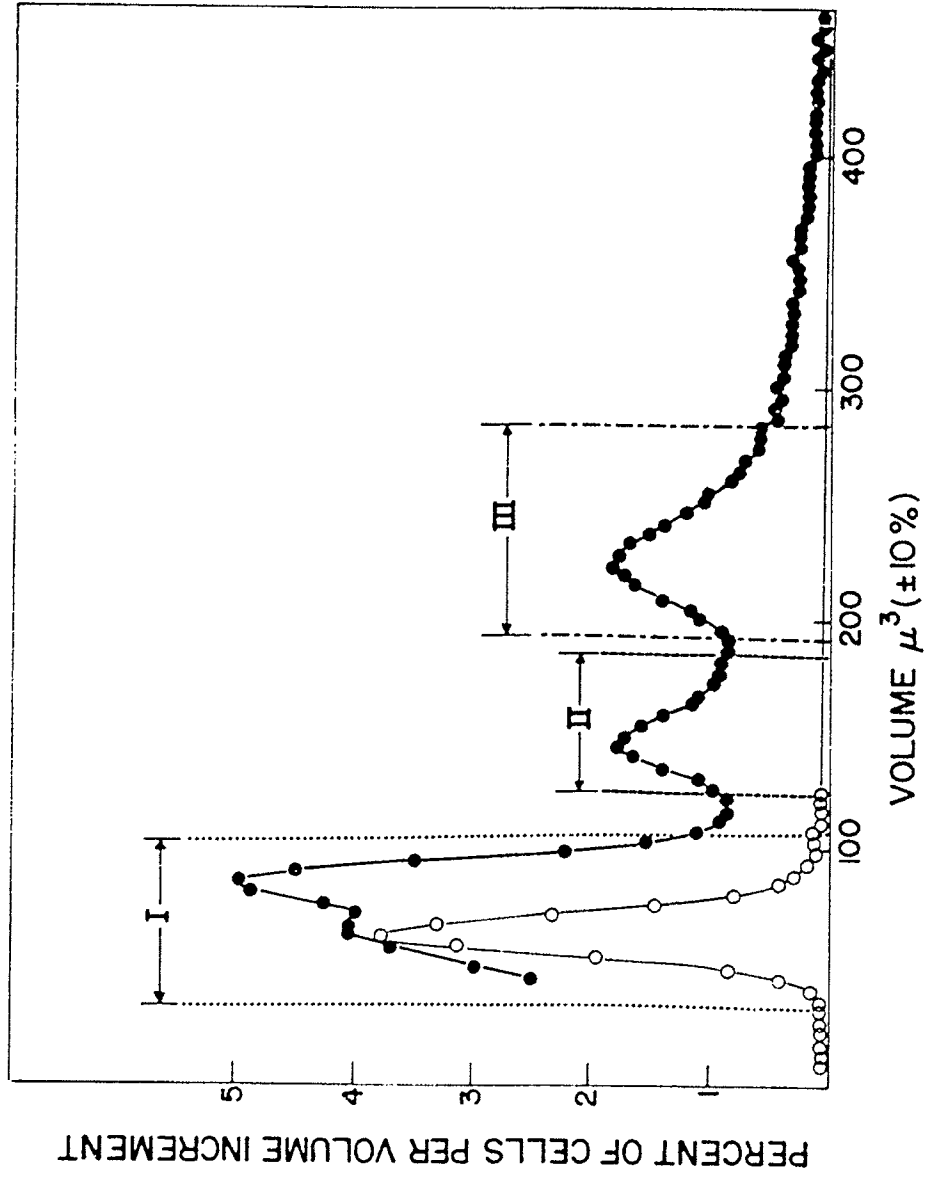


Fig. 18. A typical volume distribution of bone marrow cells obtained from the tibia of a CBA mouse. The curve of open circles represents the distribution of whole blood and establishes a volume reference.



be quite consistent among mice of the same age, sex, and condition. In a group of 16 CBA mice, the modal value of the peak in region II was $143 \mu^3$ with a dispersion given by $S = 6 \mu^3$, and the average modal volume of the peak in region III was found to be $254 \mu^3$ with $S = 8 \mu^3$. These measurements were based on calibration of the volume spectrometer with mouse erythrocytes (approximately $60 \mu^3$ in diluent IIa).

By applying the cell separator, a frequency distribution of cell types within the volume distribution of marrow cells can be obtained. This is achieved by isolating a series of volume fractions spaced across the volume distribution. Cells of each fraction are centrifuged onto a coverslip, fixed, stained, and microscopically examined to obtain a differential count. Figure 19 presents the frequency distribution of cell types found within the volume distribution of normal mouse bone marrow cells. These curves are based on differential counts of 12 volume fractions. The ordinate has the units of percent of total cells per division where only nucleated cells having volumes greater than $110 \mu^3$ are considered. Cell types were classified according to the criteria of Puck (34).

Normal mouse spleen cells, isolated as described in the Methods section, give the volume distribution shown as a solid line in Fig. 20. For reference, the distribution of bone marrow from the same mouse is given as a broken line. Assuming that the large majority of spleen cells are lymphocytes, their modal volume is quite different from that of lymphocytes found in bone marrow.

Fig. 19. Frequency distribution of cell types in bone marrow
volume distribution as determined by volume separation and subse-
quent microscopic examination.

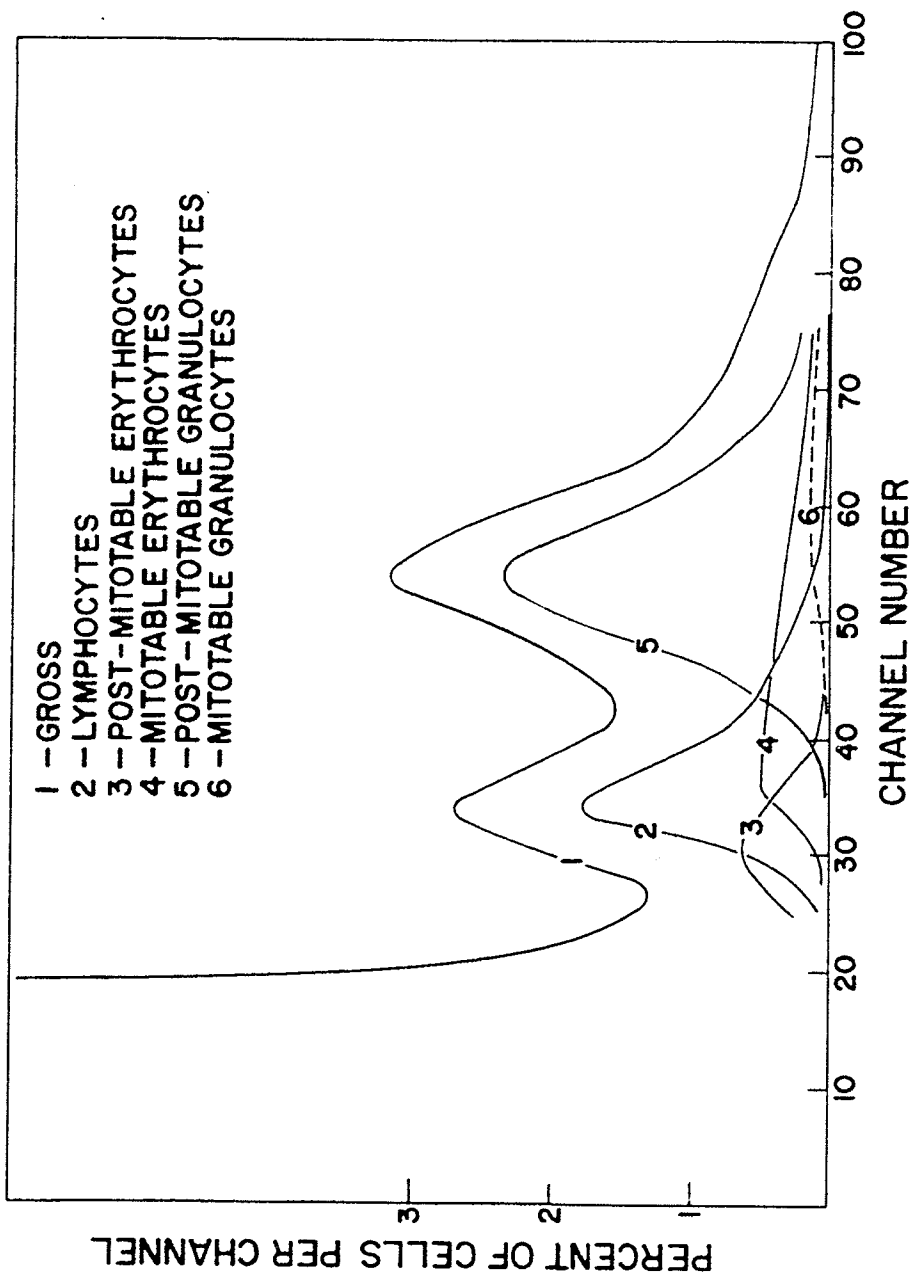
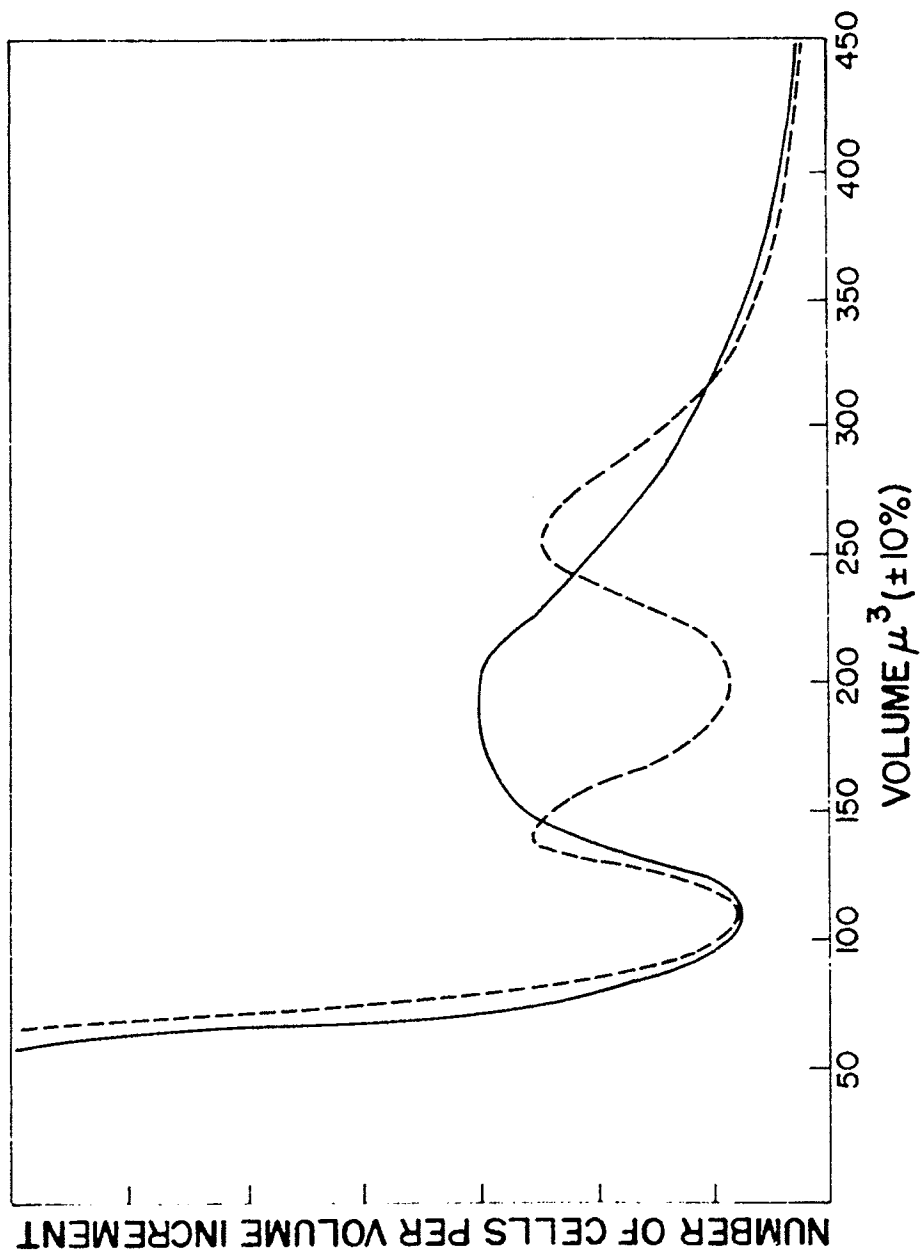


Fig. 20. Volume distribution of normal mouse spleen and marrow cells, illustrating the difference in volume of lymphocytes of the spleen and of the bone marrow.



b. Effect of X Irradiation on Volume Distribution of Bone Marrow and Spleen

During spleen depletion following whole-body X irradiation, a bimodality develops in the spleen cell distribution, as shown in Fig. 21. Here the solid line is the distribution of a normal CBA mouse spleen; the broken line is the distribution of spleen cells of a mouse 24 hours after receipt of 700 rads of 230-kV X rays to the whole body, followed by 450 rads of 230-kV X rays to the spleen region only. This bimodality can be seen as early as 4 hours post irradiation. It seems apparent that the lymphocytes of the spleen consist of 2 or more types insofar as depletion following irradiation is concerned.

- It is known that the cell population of mouse bone marrow decreases as a function of time after whole-body irradiation (36). Fifteen female CBA mice were given 500 rads of 230-kV X rays delivered to all but the right hind leg which was protected by a lead shield. At various times after irradiation marrow cells were harvested from both tibiae, and a volume distribution was obtained for each. At time zero, immediately after irradiation, 5 mice were sacrificed; the distributions of unshielded vs. shielded tibiae are nearly indistinguishable. By summing the area under the distribution curve of the left tibia and dividing by the corresponding area of the curve for the right tibia, a measure of cell loss is obtained. Figure 22 shows the marrow distributions of a mouse at 6 hours post irradiation. The 3 indicated regions were chosen for analysis. Region I includes cells having volume between $110-180 \mu^3$, region II $240-300 \mu^3$, and region III $325-378 \mu^3$. At 6 hours post irradiation,

Fig. 21. Effect of X irradiation on volume distribution of spleen cells, indicating a more rapid loss of cells in the range of 150-200 μ^3 . The distribution of a normal spleen is given as a broken line.

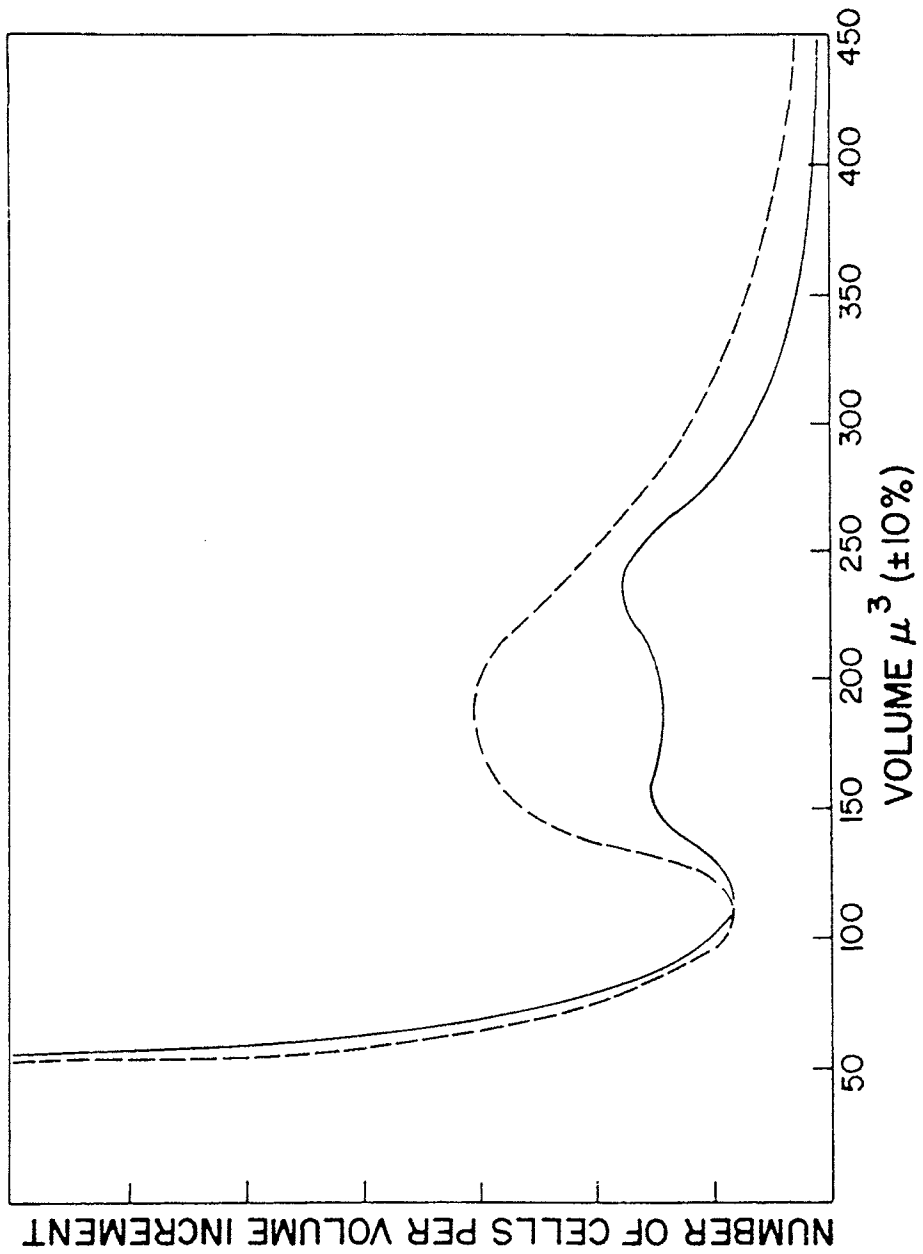
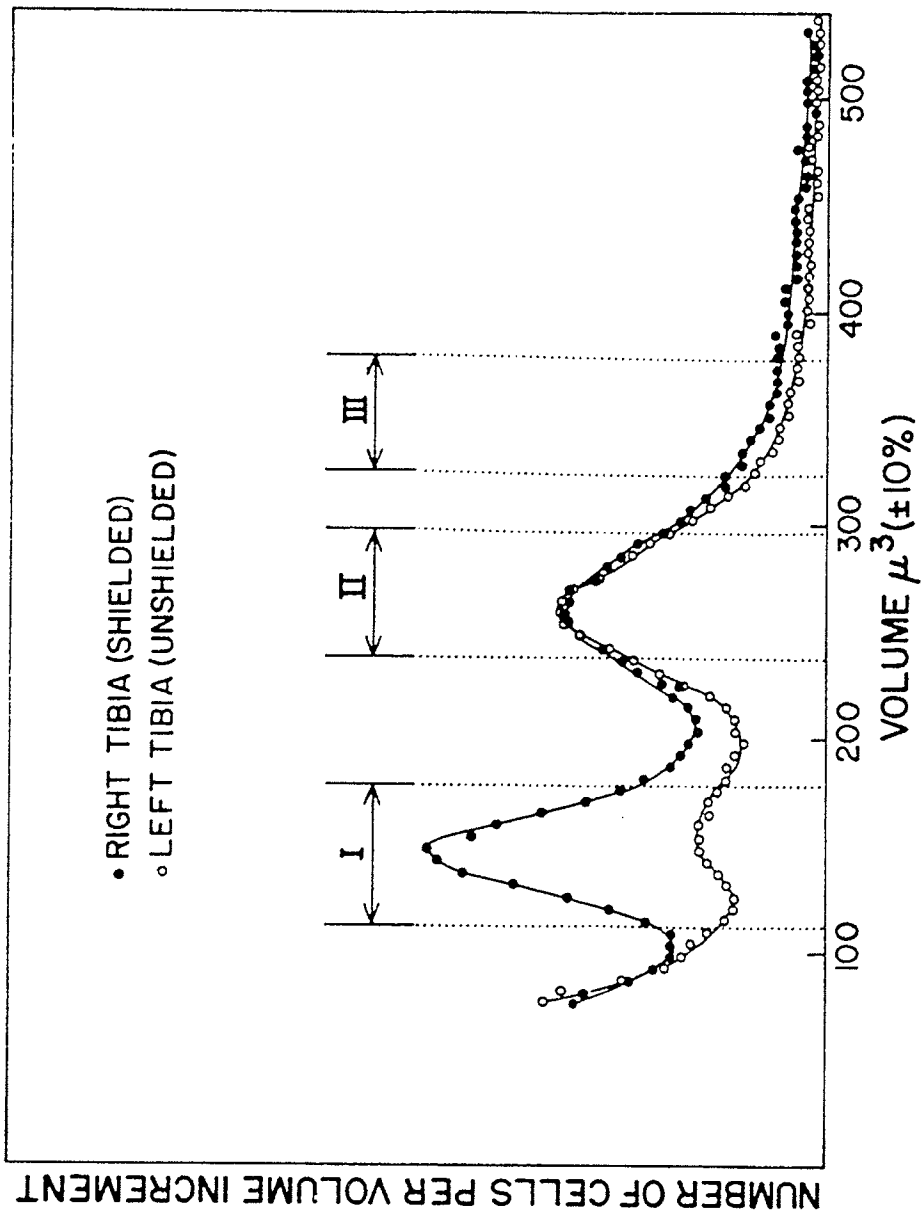


Fig. 22. Volume distributions of mouse bone marrow cells 6 hours post irradiation with 500 rads of 230-kV X rays. The right tibia was protected by lead shielding. These curves illustrate the early loss of lymphocytes.



there has been a considerable loss of cells from region I, little loss from region II, and slight loss from region III. Figure 23 is a plot of the left tibia/right tibia for the 3 volume ranges as a function of time after irradiation. Immediately following irradiation the number of cells in region I decreases, showing a 20% loss at 4 hours. Cells in regions II and III show no loss until 6 hours, beyond which the rates of cell loss are quite similar for all 3 regions ($t_{\frac{1}{2}}$ = 13.4 hours, 16.5 hours, and 10.0 hours for regions I, II, and III, respectively).

c. Colony-Forming Unites in Bone Marrow and Spleen

First described by Till and McCulloch in 1961 (33), the colony-forming unit (CFU) of mouse bone marrow has been shown to be a hemopoietic stem cell. Although considerable effort has been directed toward the problem, little success has been achieved in characterizing the responsible cell. Because of this need, an attempt was made to determine the volume of the CFU using the electronic cell separator. With this information in hand, perhaps the CFU could be associated with a bone marrow cell type by demonstrating a common cell volume.

Using the methods described above, marrow cells were obtained from CBA mouse tibiae or femora. A volume distribution of the cell suspension was obtained, and volume ranges of interest were isolated and injected into host mice. After approximately 7 days, these mice were sacrificed and their spleens scored for colonies. A typical experiment is shown in Fig. 24. The volume distribution of cells from the tibiae of a 10-week-old female CBA mouse is given as a solid

Fig. 23. Bone marrow cell loss (unshielded tibia/shielded tibia)
after receipt of 500 rads of 230-kV X rays. The 3 indicated regions
refer to those of Fig. 22.

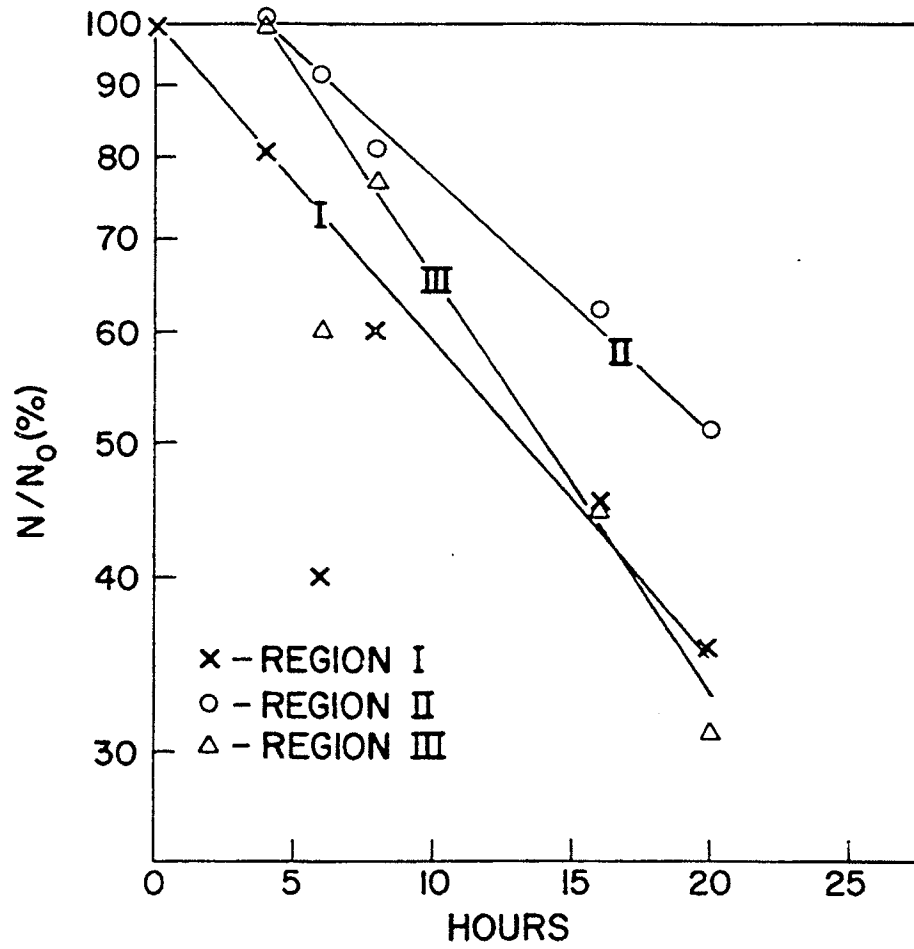
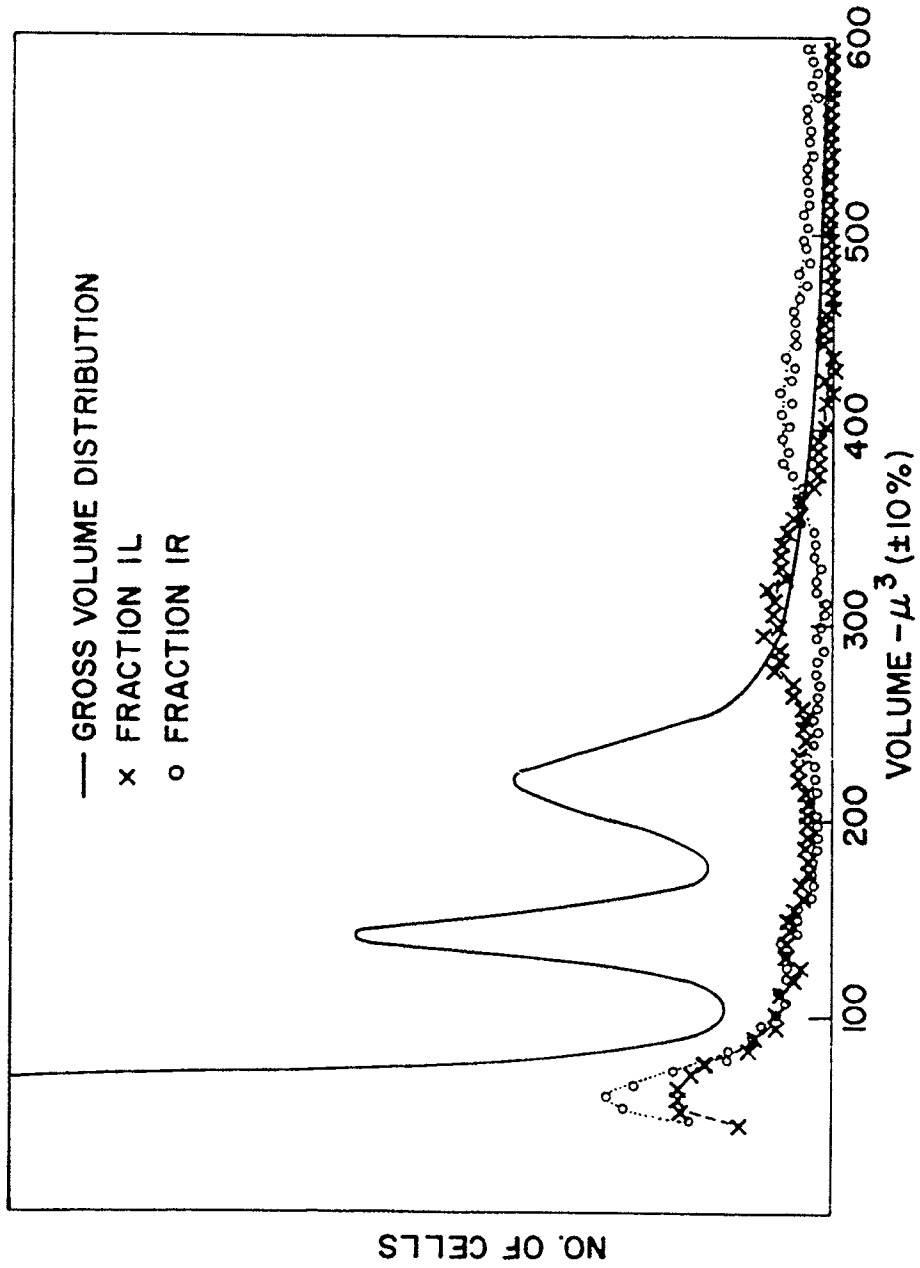


Fig. 24. Volume distributions of the gross marrow cell suspension and the 2 isolated fractions 1L and 1R which were assayed for CFU content.



line. For this fractionation, the cell separator was adjusted to remove cells of volume 260-370 μ^3 (fraction 1L) and of volume 370-600 μ^3 (fraction 1R). Approximately 2×10^5 cells were collected in fraction 1L and 1.6×10^5 cells in fraction 1R. A portion of each isolated fraction was removed and analyzed on the volume spectrometer, giving the distributions shown; the distribution of gross marrow is given for reference. A second aliquot of each fraction was centrifuged onto coverslips for cytological analysis, and the remainder was then injected into irradiated host mice to obtain CFU titer. In a subsequent run, using the same gross bone marrow suspension, 2 additional fractions were isolated. Distributions of these are presented in Fig. 25. Fraction 2L, containing approximately 2×10^5 cells from 130-165 μ^3 , consists primarily of lymphocytes. Fraction 2R contained 1.6×10^5 cells of volumes between 200 and 260 μ^3 . CFU titers were obtained on all of these fractions and on the gross cell suspension which had not been passed through the separator. An expression for the percent of total CFU found within a separated fraction is given by $\frac{\text{titer of separated fraction}}{\text{titer of gross}} \times \% \text{ of cell population}$ lying within the volume range of the fraction. Approximately 37% of the total nucleated cell population lies within the volume range of fraction 1R. Table II presents the differential count, CFU titer, and percent of total CFU found in the gross suspension and in each volume fraction. The majority of the CFU's was found in the volume range 200-260 μ^3 (fraction 2R). Note that this CFU abundance does not correlate with small lymphocyte abundance.

A preliminary experiment has been performed to delineate the volume of CFU's in normal mouse spleen. The spleen was removed from

Fig. 25. Volume distributions of the gross bone marrow suspension and the 2 isolated fractions 2R and 2L which were assayed for CFU content.

TABLE II
 DIFFERENTIAL COUNT, CFU TITER, AND PERCENT OF TOTAL CFU
 OF GROSS SUSPENSION AND OF FRACTIONS 1L, 1R, 2L, AND 2R

Sample	Volume Interval (μ^3)	Myeloid Mitotable (%)	Myeloid Post Mitotable (%)	Erythroid Mitotable (%)	Erythroid Post Mitotable (%)	Lymphoid (%)	CFU per 10^4 Cells	% of Total CFU
Gross	130-600	12	37	23	8	20	1.2 ± 0.3	100
Fraction 2L	130-165	1	4	12	14	68	0.3 ± 0.1	10
Fraction 2R	200-260	2	74	13	5	6	1.4 ± 0.1	51
Fraction 1L	260-370	6	50	28	13	4	1.1 ± 0.3	11
Fraction 1R	370-600	69	8	16	2	5	1.6 ± 0.3	10

a CBA mouse and dispersed into single cell suspension. Using the cell separator, a volume distribution was obtained, and 2 fractions were isolated. Fraction L contained 7.4×10^5 cells from the interval 125-190 μ^3 ; fraction R contained 6.7×10^5 cells between 180 and 430 μ^3 . The titer of the gross suspension was 0.24 CFU/ 10^4 ; fraction L contained 0.09 CFU/ 10^4 and fraction R 0.46 CFU/ 10^4 . Thus, the relative titer $\frac{\text{titer of fraction}}{\text{titer of gross}}$ of fraction L is 0.25 and of fraction R 1.9.

d. Spleen Cell Volume in AKR Mouse Leukemia

The spontaneous development of leukemia in AKR mice is accompanied by the appearance of large cells in the spleen. These large transformed cells are thought to originate in the thymus and subsequently to migrate to the spleen where they proliferate rapidly (37). An experiment was undertaken to study this kinetic process in terms of cell volume.

Using the methods for spleen cell dispersion described in the Methods section, cells were harvested from the spleen of a normal AKR mouse 10 days after it had received an intraperitoneal injection of 10^5 unfractionated leukemic cells. In this experiment the harvested cell suspension has the volume distribution shown in Fig. 26 as the curve of closed circles. A spleen cell suspension from a normal AKR mouse gives the distribution of open circles. It is readily apparent that the leukemic cells proliferating in the spleen are unusually large, ranging from 300-750 μ^3 . The cell separator was adjusted to remove 2 volume classes of cells: one from approximately 110-260 μ^3 and the second from approximately 300-800 μ^3 . Aliquots of the separated fractions were analyzed, giving the distributions of Fig. 27.

Fig. 26. Volume distributions of spleen cells from a normal and a leukemic AKR mouse, illustrating the appearance of large, abnormal cells in this disease.

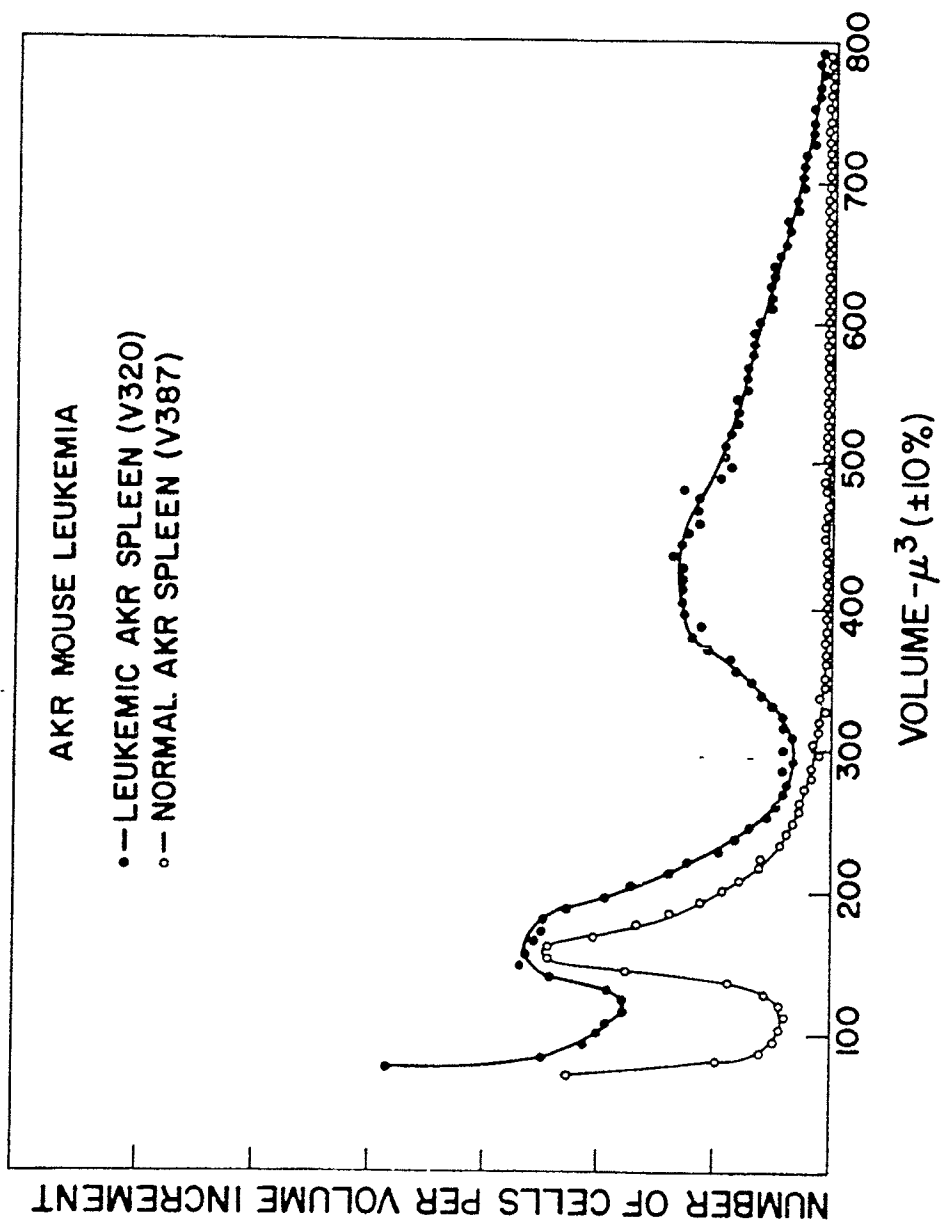
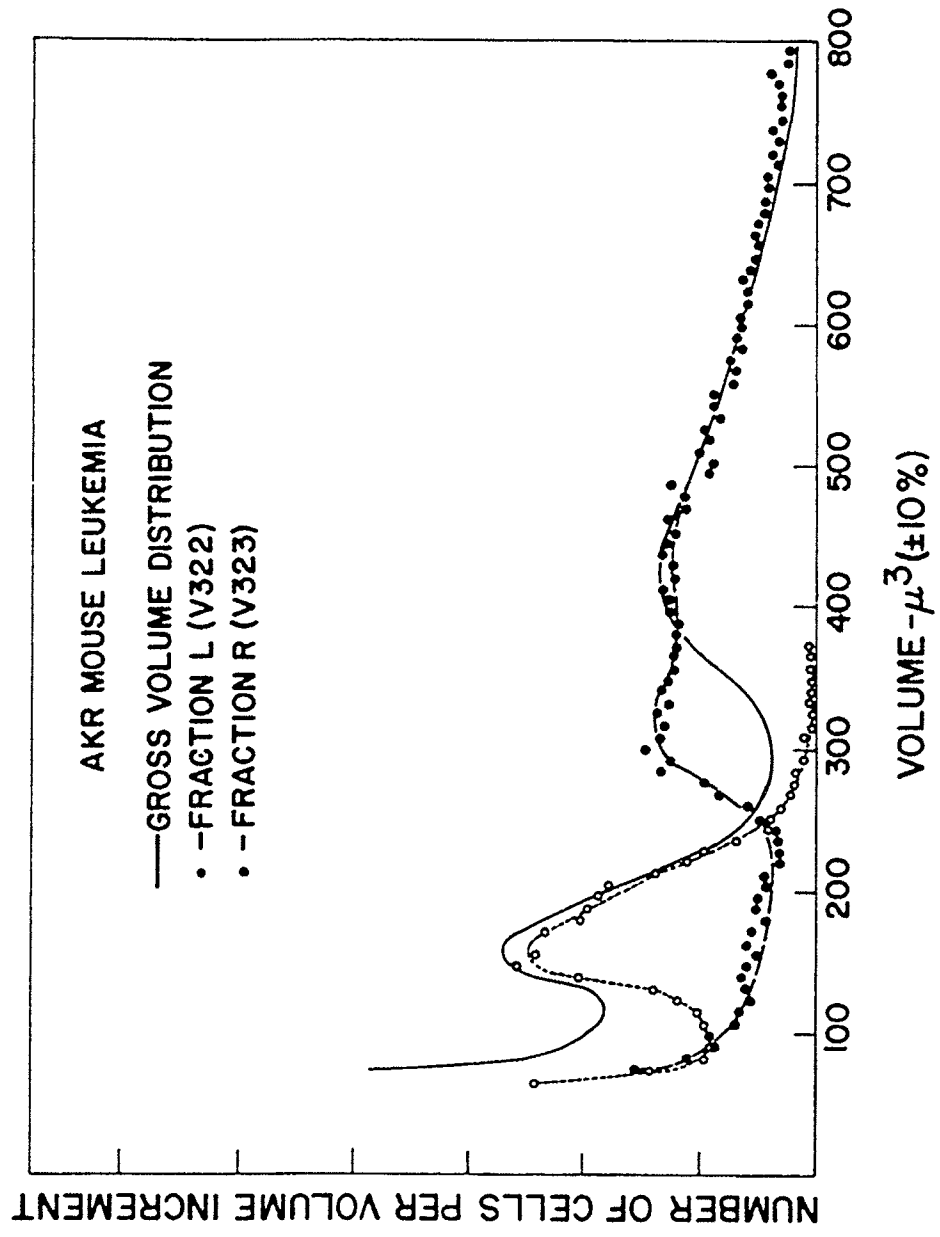


Fig. 27. Volume distributions of 2 fractions, L and R, and the leukemic cell suspension from which they were isolated. These 2 fractions were injected into normal AKR mice to determine the presence of viable leukemic cells.



Normal AKR mice received intravenous injections of cells from fraction L, fraction R, and from the unfractionated gross. The results are presented in Table III. Although still considered to be preliminary, these results have been substantiated in a subsequent experiment.

IV. DISCUSSION

A. Volume Analysis and Cell Separation

1. Minimum Sensible Volume

Passing a constant, direct current through the sensing aperture results in electrolysis of water and evolution of H_2 at the platinum disc electrode. A growing bubble of H_2 appears electronically as a particle in the aperture. If the bubbles are small when swept out by the liquid stream, the pulses produced are of small amplitude and appear as an electronic noise background which limits the ability to sense very small particles. Several orifice designs have been tried; the best to date allows resolution of particles the size of mouse red blood cells (about $60 \mu^3$) but at some sacrifice in hydrodynamic performance. Considerable effort is being directed toward this problem.

2. Resolution of Separation

An important characteristic of any technique of cell separation is the degree of homogeneity obtained. Fractions, isolated from Chinese hamster ovary cells growing in suspension culture and subsequently analyzed for volume, give distributions having coefficients of variation of approximately 10%. This estimate is somewhat too large as it incorporates 2 errors in volume measurement; the first on passing through the separator and the second in the subsequent analysis.

3. Limitation on Rate of Analysis

A fundamental limitation of this scheme is that every particle,

good or bad, must be analyzed. At present, analysis requires about 50 μ sec per particle; consequently, in order to hold to an acceptable level the probability of finding 2 particles in the aperture, the maximum analysis rate must be limited to approximately 200,000 particles per minute.

As explained earlier, the anticoincidence system acts to prevent separation if 2 sensed particles might be caught in a group of deflected droplets. However, in order for this circuit to function, the 2 particles must be electronically distinguishable (i.e., be at least 50 μ sec apart when they pass through the aperture). It may be possible to improve the time resolution of the system by differentiating the relatively long Coulter volume pulses and by using this differentiated pulse to activate the anticoincidence system. This may permit resolution of particles 20 μ sec apart; if this is achievable, the rate-limiting factor becomes the uncertainty in time of arrival of a particle at the point of droplet detachment.

4. Extension to Other Sensors

In principle, this scheme can be extended to other sensors or to a combination of sensors. Other workers have recently developed, for use with suspension flow systems, sensors for particle fluorescence (38), light-scattering ability (39), and ultraviolet absorption (40). Incorporation of these devices, perhaps in conjunction with a Coulter volume sensor, would allow separation of particles according to 2 or more simultaneously measured properties, thereby greatly increasing the ability to discriminate among cells.

Development of a separator incorporating sensors of cell volume

and cell fluorescence is underway. A potentially important application of this instrument is in the field of immunology. If sensitivity is sufficient, use of fluorescent antibody-antigen techniques might permit the isolation of cells on the basis of extremely subtle differences, detectable only by specific antibodies. For example, cells producing antibody can be specifically labeled by a two-step process. First, unlabeled, homologous antigen is added and combines with the antibody on the cell surface. In a second step, a few drops of specific, fluorescently labeled antiserum, directed against the antigen used in the first step, is added, rendering the cell fluorescent (41). Or, by using a certain cell type, these cells could be uniquely labeled and isolated from a very large, heterogeneous population. Such a dual parameter separator could be a powerful tool in the study of immune response, an area of paramount importance.

One of the criteria of cancer cell identification used in the Papanicolaou test for uterine cancer is that such cells often have an abnormally large ratio of nuclear diameter to cytoplasmic diameter (42). A measure of this property could be obtained by using a nucleus-specific fluorescent dye which, under ultraviolet excitation, would give a fluorescence signal proportional to nuclear volume. Cytoplasmic diameter is given by the Coulter volume pulse. The ratio of these signals would be electronically generated and compared with predetermined standards. Cells having a ratio outside the acceptable range would be enumerated and isolated for later microscopic examination. Such automatic procedures could greatly increase the rate of sample analysis and by analyzing many more cells per sample, increase the probability of early detection.

As described here, the device removes 2 volume fractions from a sample; however, using an earlier system of electronics, simultaneous isolation of 4 fractions has been achieved. Extension to 6 or more fractions seems quite feasible.

B. Biological Applications

1. Human Leucocytes

The volume distribution of normal leucocytes shows that lymphocytes and granulocytes are quite distinct in volume. Modal volumes of the 2 peaks were found to be quite consistent. Among 7 presumably normal male subjects the modal volume of the lymphocyte peak ranged from 250 to 265 μ^3 and the granulocyte peak from 400 to 440 μ^3 . The relative number of cells of each type (measured as the area under the curve in the range of interest) was found to fluctuate according to the health of the individual. The presence of a "cold" or other minor infection was frequently reflected. In the abnormal condition of infectious mononucleosis (Fig. 15), the lymphocytes appeared to be of a somewhat greater than normal modal volume. Abnormal cells, characteristic of this disease, appeared between the normal lymphocyte and normal granulocyte peaks, causing broadening of the peaks and shifting the modal volume of the granulocyte peak to a smaller value. Among the limited number of cases of this disease which have been studied, this volume pattern appears to be characteristic.

In acute lymphoblastic leukemia (Fig. 16), the appearance of enormous quantities of abnormally large lymphocytes is completely consistent with clinical observation. However, electronic volume analysis may be of use in the observation of hemopoietic system

response to drug therapy. In the case of chronic lymphocytic leukemia, the lymphocytes appear to be comprised of 2 populations: one having a modal volume near normal and the other, more abundant population a modal volume perhaps three-quarters that of normal. This case was diagnosed quite early in its development and probably represents a superposition of normal and abnormal hemopoiesis. These cases of abnormal human leucocytes represent the few instances in which electronic volume analysis has been applied to leucocytes in diseases involving the hemopoietic system.

2. Cell Volume in Mouse Hemopoiesis

a. Normal Mouse Bone Marrow

The modal values of the peaks in regions II and III of Fig. 18 have been found to be quite consistent among mice and to have average values of $143 \mu^3$ and $254 \mu^3$, respectively. These results compare very favorably with the values of $146 \mu^3$ and $245 \mu^3$ determined by Robinson et al. (43) using a Coulter Counter calibrated with rat erythrocytes. Although the modal volumes of these peaks were quite stable, the relative numbers of cells in each peak were found to be variable and to be highly responsive to stresses such as infection or ionizing radiation. The frequency distribution of cell type within the volume distribution of bone marrow cells (Fig. 19) provides a correlation of cell type and volume, permitting interpretation of such changes.

b. Effect of X Irradiation on Bone Marrow and Spleen

Based on the cell type curves of Fig. 19, it seems likely that

the loss of cells from region I of Fig. 22 ($110-180 \mu^3$) corresponds to an immediate loss of lymphocytes. This was verified by separating a fraction of volume $120-170 \mu^3$ (within region I) from the marrow cell suspension 16 hours after irradiation. Within this fraction the abundance of lymphocytes was considerably decreased, the number of post-mitotable erythrocytes was relatively unchanged, and the number of mitotable erythrocytes was diminished.

There is some suggestion that the lymphocytes remaining are somewhat larger than the pre-irradiation lymphocytes. This also seems to be the case with the lymphocytes of the spleen which develop, as shown in Fig. 21, a bimodal volume distribution after irradiation.

As obtained from Fig. 23, the rates of cell loss from regions I, II, and III ($t_{\frac{1}{2}} = 13.4$ hours, 16.5 hours, and 10.0 hours, respectively) are in rough agreement with an 11-hour half time for total nucleated cell loss determined by Puck (36). This latter rate, being an average rate of loss for all the cells in the marrow, would not reflect a different rate of loss among different cell types.

c. Colony-Forming Units in Bone Marrow and Spleen

As first described by Till and McCulloch in 1961 (33), hemopoietic nodules develop on the spleen of a mouse which has received a supralethal dose of X irradiation followed by an injection of bone marrow cells from an isogenic donor mouse. In view of the fact that the spleen nodules are similar in appearance to colonies formed by single cells growing in vitro, the agent responsible was given the operational designation of colony-forming unit (CFU). Later it was shown (44) that these spleen colonies did indeed develop from a

single cell possessing a proliferative capacity sufficient to produce a colony of several million cells in approximately 11 days. On close examination, it was found that these colonies contained, along with their immediate precursors, differentiated cells of the erythrocytic, granulocytic, and megakaryocytic series (45-48). Often a single colony would be found to contain a mixture of precursors and mature cells of each of these types; thus, it was suggested that the CFU was, in fact, a hemopoietic stem cell capable of commitment to divergent paths of differentiation and of self-renewal. This last postulate was given support by testing single colonies for the presence of CFU (44). On excising, dispersing, and injecting the cells of a spleen colony of a single cell type into second recipient host mice, it was found that CFU's were indeed present and that the cells of colonies subsequently produced were of an assorted nature, suggesting that this second generation CFU was also pluripotent. Consequently, to the CFU can be attributed 3 properties: 1) the capacity for extensive proliferation; 2) the ability to produce several differentiated cell types; and 3) the capacity for self-renewal.

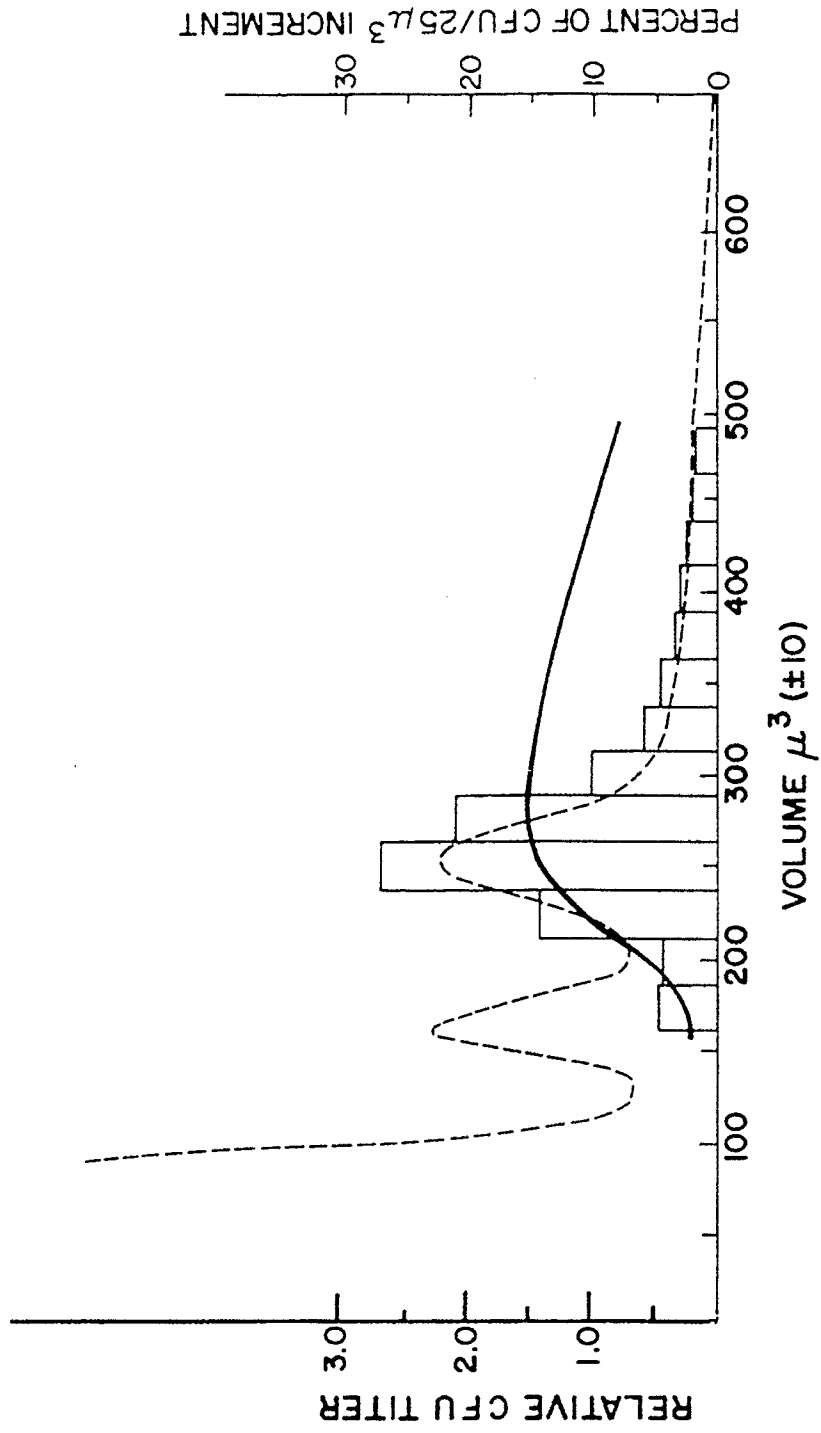
There is evidence that the direction of differentiation is determined by the microenvironment of the stem cell (46), suggesting the possibility of altering the fate of stem cell progeny through modification of stem cell environment. Because of these properties, the CFU has been the subject of great interest and investigation; unfortunately, it has not hitherto been possible to characterize the responsible cell beyond the fact that it produces a hemopoietic colony on the spleen of an irradiated host mouse. Because of its low abundance in bone marrow (approximately $2 \text{ CFU}/10^4$ total nucleated

cells), little has been learned of its morphology or physical characteristics. In an effort to characterize further the CFU, many workers have sought to define its density or to show its association with specific cell types in bone marrow (9, 50-52). It has been determined that the CFU is quite heterogeneous in density, ranging from 1.015-1.090 g/cm³ with maximum abundance reported at 1.020-1.025 g/cm³ by Niewisch et al. (52) and at 1.084 g/cm³ by Turner et al. (50). Enrichment from about 2 CFU/10⁴ nucleated cells to 6 CFU/10³ has been obtained by these workers.

It is obvious from the volume distributions that the separations shown in Figs. 24 and 25 are not ideal. Each fraction contains cells of volume smaller than the range chosen for separation. In all 4 distributions a peak can be seen in the region of 60 μ³, corresponding to the volume of mature erythrocytes. It is likely that these were isolated by 2 mechanisms: on entering the sensing disc of the separator 2 or more red cells, stuck together, would produce a particle with a volume falling within a selected range, or a red cell might stick to a larger cell (lymphocyte or granulocyte) to produce a particle within the selected range. After separation and collection, these aggregates would break up, giving the small particle contamination shown.

Figure 28 presents a composite of 6 experiments including those of figures 24 and 25 in which 16 volume fractions were isolated from mouse bone marrow and analyzed to obtain a volume distribution and CFU titer. For reference, a typical volume distribution of mouse bone marrow cells is given as a broken line. For each of these 16 fractions CFU titer was obtained and compared with that of the gross

Fig. 28. CFU abundance within the volume distribution of mouse bone marrow cells. The solid line represents the relative CFU titer $\frac{\text{titer of volume fraction}}{\text{titer of the gross}}$ and refers to the left ordinate. The histogram refers to the right ordinate and represents the percent of all recovered CFU found in $25 \mu^3$ increments between 163 and $488 \mu^3$. For reference, the volume distribution of a typical bone marrow suspension is shown as a broken line.



suspension to give a relative titer as follows: relative titer = $\frac{\text{titer of volume fraction}}{\text{titer of gross cell suspension}}$. A plot of the average relative titer as a function of volume is given as a solid line in Fig. 28 and refers to the left ordinate. This ratio is an expression for CFU enrichment, which is maximum (1.5) at approximately $270 \mu^3$.

An estimate of the percent of recovered CFU to be found in a given volume interval can be obtained by $\frac{\text{average titer in interval}}{\text{titer of gross suspension}} \times \frac{\text{number of cells in interval}}{\text{total number of cells (>120)}} = \text{relative titer} \times \% \text{ of total cells (>120 } \mu^3 \text{) in volume interval}$. Using a planimeter, the latter factor is easily determined by measuring the area under the volume distribution curve within the chosen interval and dividing by the total area under the curve and above $120 \mu^3$. The histogram of Fig. 28 is an estimate of the percent of recovered CFU's found in $25 \mu^3$ volume increments between 163 and $488 \mu^3$. CFU's are most abundant at $250 \mu^3$, and 72% are found between 212 and $312 \mu^3$.

In a preliminary fractionation of spleen cell suspension, it was found that in the range of $125-190 \mu^3$ the relative titer was 0.25 compared to a relative titer of 1.9 for the range of $180-430 \mu^3$. This preliminary experiment indicates that in the spleen, as in the bone marrow, the CFU is more abundant above $180 \mu^3$ than in the interval $125-190 \mu^3$.

It has been suggested that the CFU is a small lymphocyte (43,51, 53). While it is not possible in the work reported here to show a positive correlation between a specific cell type and CFU abundance, a negative correlation with lymphocytes is apparent. Maximum CFU abundance occurs in the volume range of $212-312 \mu^3$, whereas lymphocyte abundance is maximum between approximately 120 and $180 \mu^3$.

Niewisch et al. (52), by observing the correlation between cell types and CFU abundance, have implicated as responsible a large cell (14-17 μ diameter smear) of homogeneous overall appearance. CFU abundance did not correlate with lymphocyte abundance. In these experiments, only cells of unusually low density (1.020-1.025 g/cc) were considered. This density fraction contained only about 1% of the total CFU population.

d. Spleen Cell Volume in AKR Mouse Leukemia

In Fig. 26 it is apparent that the spleen cell volume distribution is altered by the development of early leukemia. As has been suggested by Kirsten et al. (37,54), it seems likely that this population of large cells is made up of progeny of the injected leukemic cells; if so, then these cells should induce leukemia in host mice, whereas the smaller, normal volume cells should not. This was found to be true in these preliminary experiments. Few leukemia-inducing cells are found with volume less than 300 μ^3 . Bruce et al. (55) have expressed the desirability of an assay technique which will permit enumeration of leukemic cells in the presence of nonleukemic cells. The results of these preliminary experiments suggest that electronic cell volume analysis might be developed into such a technique.

V. CONCLUSION

Electronic analysis and subsequent electronic manipulation of individual biological cells is a new concept. Because it has no close parallel in currently available techniques of cytology, the potential usefulness of this concept can be perceived only dimly. Separation on the basis of small differences in volume, while technically most easily achieved, may not be the most useful embodiment of the idea. A clearer delineation of the most fruitful direction of future development must await the experience gained in application of the device to a variety of problems.

Efforts are currently underway to improve the reliability of the device and to incorporate an existing laser-activated sensor of cell fluorescence. Because of the variety and specificity of cell fluorochromes and because of the possibilities of fluorescent antigen-antibody tagging techniques, the scope of potential applications will be greatly enlarged.

VI. FOOTNOTES AND BIBLIOGRAPHY

1. W. O. Fenn, "Effect of the Hydrogen Ion Concentration on the Phagocytosis and Adhesiveness of Leucocytes," *J. Gen. Physiol.* 5, 169-179 (1922).
2. B. L. Vallee, W. L. Hughes Jr., and J. G. Gibson, "A Method for the Separation of Leukocytes from Whole Blood by Flotation on Serum Albumin," *Blood*, Special Issue No. 1, Morphologic Hematology 82, (1947).
3. J. G. Li, and E. E. Dsgood, "A Method for the Rapid Separation of Leukocytes and Nucleated Erythrocytes from Blood or Marrow with a Phytohemagglutinin from Red Beans (*Phaseolus Vulgaris*)," *Blood* 4, 670-671 (1949).
4. S. St. George, M. Friedman, and S. O. Byers, "Mass Separation of Reticuloendothelial and Parenchymal Cells of Rat's Liver," *Science* 120, 463-465 (1954).
5. N. Coucroun, "Difference entre les electrifications de diverses varietes de bacilles Tuberculex," *Compt. rend.* 199, 165-168 (1934).
6. A. Kolin, in "Methods of Biochemical Analysis," Vol. VI., p. 259, Ed. by D. Glick, Interscience, New York, 1958.
7. E. M. Brunette, E. A. McCulloch, and J. E. Till, "Fractionation of Suspensions of Mouse Spleen Cells by Counter Current Distribution," *Cell Tissue Kinet.* 1, 319-327 (1968).
8. M. Bessis, Chap. 2, "Cytology of the Blood and Blood Forming Organs." Translated by E. Ponder, Grune and Stratton, New York, 1956.
9. J. W. Goodman, "Bone Marrow Cell Separation Studies," *Exp. Cell Res.* 21, 88-97 (1959).
10. E. A. Peterson and W. H. Evans, "Separation of Bone Marrow Cells by Sedimentation at Unit Gravity," *Nature* 21, 824-825 (1967).
11. M. J. Fulwyler, "Electronic Separation of Biological Cells by Volume," *Science* 150, 910-911 (1965).
12. L. A. Kamantsky and M. R. Melamed, "Spectrophotometric Cell Sorter," *Science* 156, 1364-1365 (1967).
13. W. H. Coulter, "High Speed Automatic Blood Cell Counter and Cell Size Analyzer," *Proc. Nat. Elec. Conf.* 12, 1034-1042 (1956).

14. E. C. Gregg and K. D. Steidley, "Electrical Counting and Sizing of Mammalian Cells in Suspension," *Biophys. J.* 5, 393-405 (1965).
15. H. E. Kubitschek, "Electronic Measurement of Particle Size" *Research* 13, 128-135 (1960).
16. H. E. Kubitschek, "Electronic Counting and Sizing of Bacteria," *Nature* 192, 234-235 (1958).
17. E. C. Anderson and D. F. Petersen, "Cell Growth and Division II. Experimental Studies of Cell Volume Distributions in Mammalian Suspension Culture," *Biophys. J.* 7, 353-364 (1967).
18. Obtained from Dow Chemical Company, Midland, Michigan.
19. Volume-pulse preamplifier and amplifier schematic diagrams are available from the Los Alamos Scientific Laboratory, Drawing No. 4Y-89116.
20. Victoreen PIP, Victoreen Instrument Division, 10101 Woodland Avenue, Cleveland, Ohio.
21. Other collection systems, such as a moving strip of filter paper, may be used.
22. R. G. Sweet, "High Frequency Recording with Electrostatically Deflected Ink Jets," *Rev. Sci. Instr.* 36, 131-136 (1964).
23. Engineering drawings for the droplet generator and volume sensor are available from the Los Alamos Scientific Laboratory, Drawing No. 2Y-57315.
24. Mosaic Fabrications, Inc., 205 Chapin Street, Southbridge, Massachusetts.
25. Hewlett-Packard Model 200-CDR.
26. McIntosh Model MI-75.
27. General Radio Company Model 1531-A.
28. Krohn-Hite Model 315-AR.
29. A detailed block diagram of the control and delay logics is available from the Los Alamos Scientific Laboratory, Drawing No. 4Y-89354.
30. A charging pulse amplifier circuit diagram is available from the Los Alamos Scientific Laboratory, Drawing No. 4Y-89361.
31. R. Herbeuval, H. Herbeuval, and J. Duheille, "Technique for Demonstrating the Presence of Cancer Cells in the Blood - Leucocyte Concentration," *Triangle* 6, 47-52 (1963).

32. E. A. McCulloch and J. E. Till, "The Radiation Sensitivity of Normal Mouse Bone Marrow Cells, Determined by Quantitative Marrow Transplantation into Irradiated Mice," *Radiation Res.* 13, 115-125 (1960).
33. J. E. Till and E. A. McCulloch, "A Direct Measurement of the Radiation Sensitivity of Normal Bone Marrow Cells," *Radiation Res.* 14, 213-222 (1961).
34. T. T. Puck, in preparation.
35. M. A. Van Dilla, M. J. Fulwyler, and I. U. Boone, "Volume Distribution and Separation of Normal Human Leucocytes," *Proc. Soc. Exptl. Biol. Med.* 125, 367-370 (1967).
36. T. T. Puck, "Cellular Aspects of the Mammalian Radiation Syndrome - II. Cell Depletion in Bone Marrow, Spleen and Thymus of Young Mice," *Radiation Res.* 27, 272-283 (1966).
37. W. H. Kirsten and R. H. Dominguez, "Chromosome Studies on Transplanted and Virus-induced Lymphoid Leukemias in Rats," *Cancer Res.* 26, 816-821 (1966).
38. M. A. Van Dilla, T. T. Trujillo, P. F. Mullaney, and J. R. Coulter, "Cell Microfluorometry: A Method for Rapid Fluorescence Measurement," *Science* 163, 1213-1214 (1969).
39. P. F. Mullaney, P. N. Dean, and M. A. Van Dilla, "Light Scattering by Biological Cells and its Relation to Cell Size," Summary Reports, Third International Congress of Histochemistry and Cytochemistry, New York, N.Y., August 18-22, 1968 (Springer-Verlag, New York, 1968), pp. 186-187.
40. L. A. Kamentsky, M. R. Melamed, and H. Derman, "Spectrophotometer: New Instrument for Ultrarapid Cell Analysis," *Science* 150, 630-631 (1965).
41. M. Goldman, "Fluorescent Antibody Methods," Chap. 10, pp. 153-173, Academic Press, New York, (1968).
42. G. Papanicolaou and H. Traut, "Diagnosis of Uterine Cancer by the Vaginal Smear," The Commonwealth Fund, New York, (1943).
43. W. A. Robinson, R. R. Bradley, and D. Metcalf, "Effect of Whole Body Irradiation on Colony Production by Bone Marrow Cells in Vitro," *Proc. Soc. Exptl. Biol. Med.* 125, 388-391 (1967).
44. A. J. Becker, E. A. McCulloch, and J. E. Till, "Cytological Demonstration of the Clonal Nature of Spleen Colonies Derived from Transplanted Mouse Marrow Cells," *Nature* 197, 452-454 (1963).

45. J. H. Fowler, A. M. Wu, J. E. Till, E. A. McCulloch, and L. Siminovitch, "The Cellular Composition of Hemopoietic Spleen Colonies," *J. Cell Physiol.* 69, 65-71 (1967).
46. N. S. Wolf and J. Trentin, "Hemopoietic Colony Studies, V.- Effect of Hemopoietic Stroma on Differentiation of Pluripotent Stem Cells," *J. Exptl. Med.* 127, 205-214 (1967).
47. J. L. Curry and J. J. Trentin, "Hemopoietic Spleen Colony Studies I. Growth and Differentiation," *Develop. Biol.* 15, 395-413 (1967).
48. I. Bleiberg, M. Liron, and M. Feldman, "Studies on the Regulation of Hemopoietic Spleen Colonies," *Blood* 29, 469-480 (1967).
49. L. Siminovitch, E. A. McCulloch, and J. E. Till, "The Distribution of Colony-forming Cells Among Spleen Colonies," *J. Cell. Comp. Physiol.* 62, 327-336 (1963).
50. R. W. A. Turner, L. Siminovitch, E. A. McCulloch, and J. E. Till, "Density Gradient Centrifugation of Hemopoietic Colony-forming Cells," *J. Cell. Comp. Physiol.* 69, 73-81 (1967).
51. G. Cudkowicz, A. C. Upton, L. A. Smith, D. G. Gosslee, and W. L. Hughs, "An Approach to the Characterization of Stem Cells in Mouse Bone Marrow," *Ann. N. Y. Acad. Sci.* 114, 571-585 (1964).
52. A. Niewisch, H. Vogel, and G. Matioli, "Concentration, Quantitation and Identification of Hemopoietic Stem Cells," *Proc. Nat. Acad. Sci.* 58, 2261-2267 (1967).
53. G. Cudkowicz, M. Bennett, and G. M. Shearer, "Pluripotent Stem Cell Function of the Mouse Marrow 'Lymphocyte'," *Science* 144, 866-868 (1964).
54. W. H. Kirsten and C. E. Platz, "Early and Late Leukemias in Rats after Transplantation of Leukemic Cells from AKR Mice," *Cancer Res.* 24, 1056-1062 (1964).
55. W. R. Bruce and B. E. Mæker, "Dissemination and Growth of Transplanted Isologous Murine Lymphoma Cells," *J. Nat. Cancer Inst.* 32, 1145-1160 (1963).